IMMUNOHISTOCHEMICAL AND MOLECULAR CHARACTERIZATION OF EXTRANODAL MARGINAL ZONE B-CELL LYMPHOMA IN SALIVARY GLANDS

by

Karen E. González Torres
MAJ, DC
United States Army

A thesis submitted to the Faculty of the
Oral and Maxillofacial Oral Pathology Graduate Program
Naval Postgraduate Dental School
Uniformed Services University of the Health Sciences
in partial fulfillment of the requirements for the degree of
Master of Science
in Oral Biology

June 2016

Naval Postgraduate Dental School
Uniformed Services University of the Health Sciences
Bethesda, Maryland

CERTIFICATE OF APPROVAL

MASTER'S THESIS

This is to certify that the Master's thesis of

Karen E. González Torres

has been approved by the Examining Committee for the thesis requirement for the Master of Science degree in Oral Biology at the June 2016 graduation.

Research Committee:

Christopher G. Fielding, DDS, MS
COL, DC, USA
Program Director, Oral and Maxillofacial Pathology
Research Committee Chair
Naval Postgraduate Dental School

James T. Castle, DDS, MS
CAPT, DC, USN
Chairman, Oral and Maxillofacial Pathology
Naval Postgraduate Dental School

Robert D. Foss, DDS, MS
Staff, Head & Neck and Endocrine Pathology
Joint Pathology Center

Glen M. Imamura, DDS, MS
CAPT, DC, USN
Chairman Department of Dental Research
Naval Postgraduate Dental School

ACKNOWLEDGEMENTS

The author thanks Dr. Rachel Werner, Dr. Guanghua Wang, Dr. Robert D. Foss, and Dr. Christopher G. Fielding for their guidance and oversight of this research project. Special acknowledgement to Dr. Rachel Werner for her diligence, advice and assistance during the IRB process.

The author hereby certifies that the use of any copyrighted material in the thesis manuscript titled:

"Immunohistochemical and molecular characterization of extranodal marginal zone B-cell lymphoma in salivary glands"

is appropriately acknowledged and, beyond brief excerpts, is with the permission of the copyright owner.

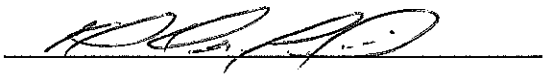

Karen E. González Torres, MAJ, DC
Oral and Maxillofacial Pathology Graduate Program
Naval Postgraduate Dental School
10 June 2016

NAVAL POSTGRADUATE DENTAL SCHOOL
KAREN E. GONZALEZ TORRES

2016

ABSTRACT

"IMMUNOHISTOCHEMICAL AND MOLECULAR CHARACTERIZATION OF EXTRANODAL MARGINAL ZONE B-CELL LYMPHOMA IN SALIVARY GLANDS"

Karen E. González Torres, MAJ, DC, USA
Master of Science in Oral Biology
Oral and Maxillofacial Pathology Graduate Program
Naval Postgraduate Dental School, 2016

Introduction: Extranodal marginal zone B-cell lymphoma (EMZBCL) is a rare, low-grade, lymphoproliferative neoplasm arising from mucosa-associated lymphoid tissue acquired from chronic antigenic stimulation. It has histomorphologic similarities with benign lesions such as lymphoepithelial sialadenitis (LESA) but has the risk of transforming into a high-grade lymphoma.

Objective: This study served as a control to validate another study evaluating previously diagnosed benign LESA lesions for a diagnosis of EMZBCL using current criteria.

Method: Nineteen cases of EMZBCL involving major salivary glands were retrieved from the Joint Pathology Center Tissue Repository and evaluated for immunohistochemical characteristics, immunoglobulin heavy chain (IgH) rearrangement and fluorescence in situ hybridization. All cases were tested for MALT1 gene rearrangement, trisomy 3 and trisomy 18. Cases with MALT1 gene rearrangement were tested for t(11;18)(q21;q21) and t(14;18)(q32;q21).

Results: Seventeen cases (9 females, 8 males; mean age of 60 years) met inclusion criteria. EMZBCL was confirmed in 15 parotid and 2 submandibular glands. All samples demonstrated lymphoepithelial lesions infiltrated by the neoplastic monocytoid B-cells.

Neoplastic B-cells were immunoreactive for CD20, CD79α in all cases but negative for CD5, CD10, CD23 and cyclin D1. BCL2 was not expressed in the germinal centers. Studies also revealed CD43 immunoreactivity (5 cases), kappa light-chain restriction (10 cases), IgH monoclonality (15 cases), increased copy number of chromosome 3 (10 cases) and increased copy number of chromosome 18 (7 cases).Two cases demonstrated MALT1 gene rearrangement, one of which also exhibited t(14;18)(q32;q21) IGH/MALT1 rearrangement and increased copy number of chromosome 3. Four cases exhibited no genetic abnormalities.

Conclusions: This study confirms current techniques used to diagnose EMZBCL and highlights the importance of considering histologic, immunohistochemical, molecular and cytogenetics studies to render an unequivocal diagnosis of EMZBCL.

TABLE OF CONTENTS

LIST OF TABLES

LIST OF FIGURES

I. REVIEW OF THE LITERATURE

Mucosa-associated lymphoid tissue (MALT) is specialized lymphoid tissue found in association with mucosal surfaces: gastrointestinal tract (gut-associated lymphoid tissue; Peyer's patches), genitourinary tract, nasopharynx and oropharynx (Waldeyer's ring - tonsils, adenoids). It consists of four lymphoid compartments: organized mucosal lymphoid tissue with germinal center formation, lamina propia, intraepithelial lymphocytes and regional lymph nodes.[1] The lymphoid follicles are similar to those encountered in lymph nodes, anatomically and immunophenotypically; however, the expanded marginal zone reaches the surface epithelium in lymphoid follicles. The interfollicular areas contain T-cells and dendritic cells. The lamina propia exhibits plasma cells, macrophages and random B and T lymphocytes. The plasma cells mainly produce immunoglobulin (Ig) A and some IgM, IgG and IgE.

The function of MALT is to detect and transport pathogens (especially infectious agents) entering the body through the mucosal surfaces into the lymphoid tissue before they have the opportunity to affect the host. Specialized epithelial cells (M cells) in mucosal epithelium recognize antigens, take them up by the process of pinocytosis and transport them to subepithelial tissues where lymphocytes reside (follicular areas containing T- and B-cells).[1] Once the lymphocytes are exposed to antigen, they may migrate to other mucosal tissues (homing process). This circulation ensures that the small number of lymphocytes specific for any given antigen has the best chance to encounter that antigen in other mucosal tissues. Sites normally devoid of native MALT such as the stomach, salivary gland (aside from intrasalivary gland lymph nodes), lung

(bronchus-associated lymphoid tissue), thyroid and ocular adnexa can acquire MALT under chronic inflammatory stimulation. The acquired MALT behaves in a similar fashion as lymph nodes; therefore, it can manifest benign lymphoid lesions and undergo malignant transformation at these extranodal sites.

Benign lymphoid lesions in the major salivary glands

In 1882, Johann von Mikulicz-Radecki, described a uniform infiltrate of small round cells (known today as lymphocytes) in enlarged lacrimal and salivary glands. This condition later became known as Mikulicz's disease.[2] In 1952, Godwin coined the term benign lymphoepithelial lesion (BLEL) to characterize a "lymphoid proliferation of the salivary glands consisting of lymphoid hyperplasia and epithelial alterations" similar to that found by Mikulicz.[3] Godwin found the term BLEL more appropriate as it did not imply that the lymphoid proliferation was exclusively inflammatory or neoplastic. In a separate study, Schmid, Helbron, and Lennert reported on lesions comparable to those described by Godwin but named them myoepithelial sialadenitis (MESA) because of their myoepithelial proliferation and lymphoid infiltration.[4] Both names, BLEL and MESA, were therefore used interchangeably for some time. The term "pseudolymphoma" was used to describe extraglandular tumor-like aggregates of lymphoid tissue that did not meet the histologic criteria for malignancy but were more than a benign lymphoepithelial proliferation.[5] The use of "pseudolymphoma" has been abandoned since it became a "catch-all" term for lesions that could not be classified as benign or malignant at the time of diagnosis. In 1999, Harris conceived the term lymphoepithelial sialadenitis (LESA) to distinguish lesions previously designated as

MESA/BLEL since it became known that the non-lymphoid cells involved in these lesions were epithelial in origin (basal epithelial cells) and not myoepithelial cells.[6] LESA was characterized by Harris (1999) as a "lymphoid infiltrate with follicular hyperplasia, surrounding and infiltrating salivary ducts, with disorganization and proliferation of the ductal epithelial cells forming lymphoepithelial lesions (LELs)" (previously known as epimyoepithelial islands) .[6] LESA is the term still in use today.

LESA is a non-neoplastic, reactive lesion characterized by unilateral or bilateral enlargement of the major or minor salivary glands and/or lacrimal glands.[7] It is most commonly seen in females between 40 and 70 years of age and primarily involves the parotid gland.[7] The clinical presentation is a diffuse, firm, unilateral swelling of the affected gland with or without pain. Since normal salivary gland does not contain extranodal lymphoid tissue, the development of LESA represents acquired MALT. In addition to the microscopic features described by Harris (1999)[6], histologic evaluation of LESA also reveals effacement of the affected gland parenchyma with preservation of the overall lobular architecture, atrophy of glandular and ductal epithelium, cystic alterations of the LELs, collection of hyaline material in the LELs and germinal center formation in the polyclonal lymphocytic infiltrate.[7, 8] The lymphocytes infiltrating the epithelial proliferations (LELs) tend to be larger than those present in the stromal lymphoid infiltrate. They are predominantly B-cells and exhibit features of monocytoid B-cells or centrocyte-like cells (small, atypical cells resembling centrocytes, but with more abundant cytoplasm).[9] The surrounding lymphoid infiltrate consists primarily of

mature T lymphocytes.[9] The development of LELs in acquired MALT is indicative of a lymphoproliferative disorder.[10]

Patients with LESA usually suffer from Sjögren syndrome (SS) and have a forty four fold increased risk of developing salivary gland lymphomas.[7, 11] The primary lesion to consider in the differential diagnosis of LESA in the salivary glands is a MALT-derived lymphoma. Benign lymphoid lesions observed in salivary glands that could potentially be mistaken for LESA include but are not limited to chronic sclerosing sialadenitis, reactive follicular hyperplasia, HIV-associated salivary gland disease, lymphoepithelial cyst and lymphadenoma (nonsebaceous).

Chronic sclerosing sialadenitis (also known as Küttner tumor) is an inflammatory process seen in the salivary glands. It is most common in the submandibular gland[9] of older adults. A firm swelling is clinically seen, usually due to ductal obstruction from a sialolith. Viral, bacterial and noninfectious causes (radiation therapy, SS) have also been identified.[12] Histologically, mild, focal, periductal chronic inflammation, ductal ectasia and periductal fibrosis are evident. The chronic inflammatory infiltrate is mainly composed of lymphocytes but plasma cells can also be seen. As the lesion progresses, marked acinar atrophy with preservation of the lobular gland architecture and extensive fibrosis are noted. No LELs are identified.

In reactive follicular hyperplasia there is marked proliferation of hyperplastic lymphoid follicles with prominent germinal centers, most commonly caused by bacterial infection.[13] Patients exhibit localized or generalized lymphadenopathy with or without systemic symptoms such as fever, malaise and fatigue. Histologic features include

numerous enlarged follicles in which polarized central germinal centers are composed of a mixed population of centroblasts (large, non-cleaved activated B-cell which enlarges and proliferates in the germinal center of a secondary lymphoid follicle), centrocytes (small cleaved follicular center B-cells formed after centroblasts cease to proliferate), T-cells, follicular dendritic cells and tingible-body macrophages.[13] A well-demarcated mantle zone surrounds the germinal centers. Absence of monoclonality of immunoglobulins or known molecular aberrations seen in lymphomas differentiate this lesion from a malignant process. LELs are not identified.

As its name implies, HIV-associated salivary gland disease (also known as multiple lymphoepithelial cysts of the parotid gland; cystic lymphoid hyperplasia) is seen in HIV-infected individuals. It is characterized by xerostomia and/or unilateral or bilateral enlargement of one or more major salivary glands. Males are most commonly affected. Parotid gland involvement is found in 98% of cases followed by the submandibular gland (2%).[7] HIV-associated salivary gland disease is usually seen early in the disease prior to the development of acquired immune deficiency syndrome (AIDS). Microscopic evaluation reveals multiple cysts lined by squamous epithelium and LELs permeated by a dense lymphocytic infiltrate. Follicular hyperplasia of lymphoid tissue with prominent, irregular germinal centers and multinucleated giant cells are appreciated, especially in the parotid gland. Multinucleated giant cells or alterations of lymphoid follicles are not evident in LESA.[8]

Lymphoepithelial cysts are unilateral (mostly) or bilateral benign lesions of the salivary glands which present clinically as an asymptomatic, painless swelling. Males are

affected more often than females.[7] Histologic evaluation reveals a unilocular cyst lined by squamous, cuboidal or columnar epithelium. The cyst wall contains a dense lymphocytic proliferation which usually exhibits germinal center formation. The lesion is well delineated from the gland parenchyma by fibrous tissue. LELs and multinucleated giant cells are not identified.[8] The lymphoid component in the cyst wall does not permeate the epithelial cyst lining.

Lymphadenomas (nonsebaceous) occur mostly in the parotid gland of older adults as an asymptomatic, painless mass. Histologic evaluation reveals numerous islands, cysts and duct-like structures scattered throughout a dense lymphocytic stroma with germinal centers.[9] The cystic areas tend to exhibit intraluminal proteinaceous material, to include keratin. If keratin-filled cysts rupture, a foreign body giant cell reaction may be evident. The lymphocytic stroma does not infiltrate the epithelial component. Lymphadenomas do not infiltrate adjacent parenchyma but show a pushing border.[8]

Malignant lymphoid lesions in the major salivary glands

Primary malignant lymphomas can be classified as Hodgkin lymphomas (HL) or non-Hodgkin lymphomas (NHL). The majority of HL occur in nodal sites while 48% of NHL occur in extranodal sites.[14] NHL have a worse prognosis than HL. Most lymphomas originating in the head and neck are NHL, accounting for 75% of lymphomas in this area.[14] In salivary glands, most lymphomas (84%-94%) are B-cell NHL while only 4% of Hodgkin lymphomas have been reported exclusively in the parotid gland.[7, 15, 16, 17] They

can arise *de novo* or in the setting of immune sialadenitis (progression of LESA into malignant lymphoma).

Primary malignant lymphomas of salivary glands represent less than 5% of all primary extranodal NHL and about 2% of all salivary gland tumors.[7] They are most often found in the parotid gland (70%) followed by the submandibular gland (25%), minor salivary glands and sublingual gland (2% for the latter two combined), in order of frequency.[6, 18, 19] When arising in the major salivary glands, a lymphoma can originate within paraglandular lymph nodes from which it invades the stroma or within the glandular stroma itself. In either case, the lymphoma is considered a primary extranodal lymphoma if there is no evidence of disease outside the salivary gland[19] and if it is not confined only to the paraglandular lymph nodes[20], in which case it would be classified as a nodal lymphoma. Prior to the diagnosis of a primary malignant lymphoma in the salivary glands, involvement by lymphoma of any other site of the body must be ruled out.

The most common primary malignant lymphoma of the salivary glands is MALT lymphoma followed by diffuse large B-cell lymphoma (DLBCL) and follicular lymphoma.[14] Even though mantle cell lymphoma, anaplastic large cell lymphoma, extranodal NK/T-cell lymphoma of nasal type, peripheral T-cell lymphoma and Hodgkin lymphoma have been reported in the salivary glands, their incidence is so rare that discussion of such entities is beyond the scope of this review. In addition to characteristic morphologic appearance during microscopic evaluation, immunohistochemical (IHC) staining techniques facilitate distinguishing the aforementioned types of lymphomas from one

another and from benign lymphoid lesions such as LESA (see Table 1 for a description of IHC stains commonly used).

Table 1. Commonly Used IHC Stains to Diagnose Lymphoproliferative Lesions			
IHC	**Description**	**Immunoreactivity (+)**	**Staining pattern**
CD3	T-cell receptor[13]	T-cell lineage–specific antigen[21]	membranous and cytoplasmic[21]
CD5	T-cell surface glycoprotein[13]; loss of this marker may be seen as one of the first findings in a developing T-cell lymphoma[21]	majority of peripheral (mature) T-cells[21]	membranous[21]
CD10	neutral endopeptidase[13]	all cells derived from pre-B lymphocytes; follicular center (germinal center) cells[22]	membranous[22]
CD20	non-glycosylated, membranous phosphoprotein; acquired by late pre-B-cells as they mature; typically lost when B-cells become plasma cells[21]	B-cell lineage[21]	membranous[21]
CD23	B-cell growth and activation factor[22]	dendritic cell and B-cell marker[22]	membranous[22]
CD30	tumor necrosis factor[13]	normal activated T- and B-cells; virally transformed B- and T- cells; monocytes, macrophages, granulocytes[21]	membranous or paranuclear[21]
CD43	sialoglycoprotein on surface of human T lymphocytes, monocytes, granulocytes and some B lymphocytes[13]; plays role in regulation of hematopoiesis[21]; not expressed in normal B-cells	hematopoietic precursors; mature white blood cells in the periphery; tissue macrophages, dendritic cells, smooth muscle cells, epithelium, endothelium, myeloblasts, lymphoma cells, metastases of solid neoplasms[21]	cytoplasmic[21]
CD45	leukocyte common antigen[13]; regulator of T- and B-cell antigen receptor-mediated activation[22]	hematopoietic cells except mature red blood cells, platelets or megakaryocytes[22]	membranous and cytoplasmic[21]
CD79α	B-cell marker with broadest sensitivity[21]	B-cell lineage[21]	cytoplasmic[21]
cyclin D1	protein with cell cycle regulatory functions[13]; regulator of cell cycle progression (G1 to S-phase)[13]	mantle cell lymphoma; not expressed in non-neoplastic lymphoid cells[21]	nuclear[21]
BCL2	suppresses apoptosis in various cell systems[13]; expression should not be interpreted as evidence of malignancy[21]	intrafollicular T-cells, T- and B- cells in the interfollicular areas, primary follicles, mantle zone B-cells[21]	membranous[21]

BCL6	encodes protein thought to play a role in B-cell differentiation within the germinal center[21]	B-cells of germinal center origin[21]	nuclear[21]
EBER	Epstein-Barr virus (EBV) encoded RNA[13]	EBV	nuclear
MUM1[0]	interferon regulatory factor four[13]; encodes transcription factor responsible for development in B-, T-, plasma, dendritic, and myeloid cells[21]	non-specific; non-neoplastic "activated" T-cells, a subset of germinal center B-cells, normal melanocytes[21]	nuclear and cytoplasmic[21]
PAX5[1]	B-cell–specific activator protein; commit B-cell progenitors to the B-cell lineage by suppressing non–B-cell–associated genes and activating B-cell–specific genes[21]	early B-cell precursors, mature B-cells, Reed-Sternberg cells characteristic of Hodgkin lymphoma[21]	nuclear[21]
Kappa (κ)	immunoglobulin light-chain[22]; 2:1 kappa:lambda ratio is normal[22]	restricted expression suggests monoclonality and a neoplastic process[22]	cytoplasmic
Lambda (λ)	immunoglobulin light-chain[22]; 2:1 kappa:lambda ratio is normal[22]	restricted expression suggests monoclonality and a neoplastic process[22]	cytoplasmic
Ki-67	marker of cell proliferation[13]	low/high proliferation index	nuclear[22]
[0]MUM1 = melanoma-associated antigen (mutated) 1 gene [1]PAX = paired-box containing family of transcription factors			

Extranodal DLBCL occurs in 40% of extranodal lymphoma cases, most frequently in the gastrointestinal tract.[18] In salivary glands, extranodal DLBCL accounts for 10% of primary malignant NHL lymphomas, with 75% of the cases occurring in the parotid gland and 20% of the cases occurring in the submandibular gland.[7, 16] Most cases arise *de novo* but some cases represent transformation from an underlying low-grade lymphoma (i.e. extranodal marginal zone B-cell lymphoma (EMZBCL), follicular lymphoma).[16] DLBCL is an aggressive neoplasm with a variable clinical course. Extranodal DLBCL occurs in older men more often than females.[18] The most common clinical presentation is a painless swelling of the involved salivary gland and a firm, nontender mass. The neoplastic cells are large and dyscohesive, characterized by pleomorphism, enlarged nuclei (twice as large as a small lymphocyte), prominent eosinophilic nucleoli and vesicular chromatin. These malignant cells infiltrate the gland parenchyma replacing the

ductal and acinar components and causing effacement of the normal lobular architecture. Increased mitotic activity to include atypical mitoses is observed. LELs are not existent.[7] Even though it can vary, the characteristic IHC profile of DLBCL is as follows (Table 2): CD10+, CD20+, CD45+, CD79α +, PAX5+, BCL6+, MUM1+, CD3-, CD23-, BCL2-, EBV-, cyclin D1- and variable for CD5, CD30 and CD43.[1, 7, 8, 13, 16] The proliferation index is moderate to high as demonstrated by the antibody Ki-67 (>20%).[7] Epithelial, melanocytic and neuroendocrine markers are negative. The 5-year survival rate is 50%.[18]

Table 2. Characteristic IHC Profile of DLBCL and Follicular Lymphoma

IHC	CD5	CD10	CD20	CD23	CD43	CD45	CD79α	Cyclin D1	BCL2	BCL6	MUM-1	PAX-5	EBV	Ki-67
DLBCL	V	+	+	-	V	+	+	-	-	+	+	+	-	H
FL	-	V	+	+	-	+	+	-	+	+	V	+	-	L

V = variable H = high L = low FL = follicular lymphoma DLBCL = diffuse large B-cell lymphoma

Primary extranodal follicular lymphomas are most commonly seen in the skin but are also observed in the gastrointestinal tract, thyroid, testicles, ocular adnexa, breast and, rarely, salivary glands.[13, 16] The age at diagnosis is usually in the sixth decade of life. Nakamura (2006) reported that follicular lymphoma in salivary glands occurs at a younger age than EMZBCL.[15] The parotid gland is affected most commonly than the submandibular gland. Extranodal follicular lymphomas usually arise *de novo* and are not induced by chronic inflammation or autoimmune disease like EMZBCL.[23] They present as a firm swelling of the affected gland. Histologically, extranodal follicular lymphomas exhibit similar features as nodal follicular lymphomas. Microscopic examination reveals

a mixture of centrocytes and centroblasts in the center of the follicles, atrophy of acini and salivary ducts, lack of a fibrous capsule, lack of tingible-body macrophages (seen in reactive lymph nodes), loss of polarization of germinal centers, low mitotic activity and absence of a well-defined mantle zone.[15, 16, 23] LELs may be present. There is a tendency for transformation into high-grade lymphoma, primarily DLBCL. IHC (Table 2) demonstrates immunoreactivity for CD79α, CD20, CD23, CD45, BCL2 (within germinal centers), BCL6 and PAX-5.[15, 16, 18, 23, 24] CD 23 and CD43 highlight the dendritic mesh network only. No immunoreactivity is observed for CD3, CD5, cyclin D1and EBV.[15, 16, 18] CD10, CD30 and MUM1 exhibit variable immunoreactivity.[13, 22] Light-chain restriction (κ or λ) is commonly seen and Ki-67 is usually low. The main genetic alteration in extranodal follicular lymphoma is t(14;18)(q32;q21), resulting in the rearrangement of the BCL2 gene and consequent anti-apoptotic mechanism.

Extranodal Marginal Zone B-cell Lymphoma of MALT (MALT lymphoma; EMZBCL)

In 1971, Azzopardi and Evans reported the development of malignant lymphoma in the parotid gland arising in patients with Mikulicz's disease.[25] In 1976, Nime, Cooper, and Eggleston described primary malignant lymphoma of the salivary glands as a "lymphomatous infiltrate showing poorly differentiated lymphocytes and malignant histiocyte-like cells".[26] In 1983, Isaacson and Wright first introduced the term MALT-derived lymphoma instead (concept of EMZBCL), referring to an indolent, localized, low-grade extranodal B-cell NHL arising in gastric MALT.[27] It was characterized as a lymphoma of follicle center cell (FCC) origin with plasma cell differentiation, which localizes around, invades, and destroys epithelial structures.[28] They observed that MALT

lymphomas found in locations other than the gastrointestinal tract (i.e. lung, thyroid, salivary glands, ocular adnexa) had similar behavior as gastric MALT: localized formation of LELs surrounded by B-cells, infiltration of glandular tissue by neoplastic B-cells and tendency to remain localized for long periods of time.[28] In 1994, the International Lymphoma Study Group accepted the term marginal zone B-cell lymphoma, extranodal, MALT-type to describe a lymphoma composed of marginal zone/monocytoid (centrocyte-like) cells, lymphocytes, plasma cells, LELs infiltrated by marginal zone cells, occasional centroblasts and reactive follicles with the neoplastic marginal zone or monocytoid B-cells occupying the marginal zone and or the interfollicular region.[29] By 2008, the World Health Organization (WHO) included the extranodal marginal zone B-cell lymphoma of MALT (MALT lymphoma/EMZBCL) in its classification to refer to a primary extranodal lymphoma composed of morphologically heterogeneous small B-cells (marginal zone cells, lymphocytes, centroblast-like cells) and in which the neoplastic cells spread out and infiltrate the epithelium forming large confluent areas recognized as LELs.[16] Primary EMZBCL lesions (MALT lymphoma) arising in the major salivary glands will be characterized in this study.

MALT lymphomas are low-grade, small cell lymphomas comprising 7.6% of all NHL.[16, 30] They are sub-classified as EMZBCL, nodal MALT lymphoma and splenic MALT lymphoma. Most EMZBCL occur in the stomach (58%) but can affect any organ in the body: lung (14%), head and neck (14%), salivary glands (14%), ocular adnexa (12%), skin (11%), thyroid (4%) and breast (4%).[16, 18, 30, 31] They usually arise from lymphoid tissue acquired by chronic antigenic stimulation triggered by persistent infections and/or

autoimmune processes.[28, 30, 31, 32] Therefore, MALT lymphomas can be seen in association with Sjögren syndrome, hepatitis C infection, Hashimoto thyroiditis, *Helicobacter pylori* infection in the gastrointestinal tract, *Chalmydophila psittaci* infection in ocular adnexa and *Borrelia burgdorferi* infection in cutaneous sites.[16, 33] A chronic infectious etiology is illustrated by the fact that gastric MALT lymphoma regresses in 75% of cases after eradication of *Helicobacter pylori* with antibiotics.[13]

MALT lymphoma (EMZBCL) of salivary glands represents 14% of extranodal lymphoma cases.[18] It presents in the parotid gland in 75% of the cases and in the submandibular gland 20% of the cases.[7, 15, 20] In salivary glands, EMZBCL arises most often in females in a wide age distribution, predominantly during the seventh decade.[7, 13] It predominates among Hispanics and its incidence increases with age.[34] EMZBCL of salivary gland presents as a slow growing, painless mass with or without cervical lymphadenopathy. It most commonly arises in MALT acquired secondary to LESA as evidenced by the fact that 85% of lymphomas in patients with Sjögren syndrome/LESA are MALT lymphomas.[1, 16] Not all cases of LESA progress to EMZBCL.[35] Which cases of LESA will progress to EMZBCL cannot be predicted. Disease progression has been hypothesized as follows: (1) chronic stimulation of polyclonal B-cells at the affected site from which a monoclonal population arises, (2) acquisition of chromosomal abnormalities inducing MALT lymphoma, and (3) potential transformation to high-grade lymphoma.[33] A transformation from low-grade EMZBCL to a high-grade lymphoma has been observed mainly in patients older than 60 years old and with lymph node

involvement at time of presentation.[33, 36] Transformation to diffuse large B-cell lymphoma is well-documented.[32]

Histologically, EMZBCL is characterized by an expansile, diffuse, and destructive infiltrate of marginal zone (monocytoid, centrocyte-like) B-cells with irregular nuclei and distinct rims of clear cytoplasm.[31] The LELs are formed by infiltration of the neoplastic cells into the glandular tissues, resulting in disruption, obliteration and effacement of glandular and ductal architectures.[31, 32] LELs tend to be prominent with large aggregates of marginal zone/monocytoid B-cells with abundant cytoplasm.[31] The marginal zone/monocytoid B-cells (centrocyte-like) are also found outside the LELs forming broad halos around the LELs or forming broad anastomosing strands between the LELs.[6] Plasmacytic differentiation may or may not be observed around the LELs.[31, 37] When present, the plasmacytic differentiation forms a band-like infiltrate of normal, mature plasma cells which may have Dutcher bodies within the nuclei.[31] Lymphoid cells and plasma cells (when present) express monotypic/monoclonal surface immunoglobulin and do not tend to infiltrate the LELs.[11] Demonstration of monotypic immunoglobulin (Ig) light-chain expression (κ or λ) confirms a diagnosis of malignant lymphoma.[31] Large centroblast-like cells are present as a minor component of the neoplastic process[16] and reactive germinal centers are frequently seen.[32] Not all histopathologic features need to be observed in order to make the diagnosis. Immunophenotyping should be part of the diagnostic work up to reach an unequivocal definitive diagnosis.

EMZBCL of the salivary glands shows immunoreactivity (Table 3) for CD20 and CD79α, supporting its B-cell origin[6, 32, 33, 38] Immunoreactivity for BCL2 and PAX-5 are

also observed.[13] κ or λ light-chain restriction and Ig heavy chain rearrangement are usually seen.[13] CD3, CD5, CD10, CD45, BCL6, cyclin D1and EBV fail to immunoreact in EMZBCL.[6, 13, 31, 32, 33, 37, 38, 39, 40, 41, 42] Variable reactivity has been documented with CD23 and CD43 (positive in 30-50% of cases), which highlight the dendritic mesh network and a subset of activated B-cells, respectively.[6, 9, 13, 31, 32, 39, 43] MUM1 immunoreactivity is observed in the plasma cell component, when present.[16] The proliferation index is low as demonstrated by the antibody Ki-67.[13, 31] Cytokeratin highlights the lymphoepithelial lesions but is negative in the neoplastic lymphoid cells. There is no specific marker for the diagnosis of EMZBCL. CD20+/CD3- reactivity confirms a diagnosis of lymphoma[40] of B-cell origin. CD5-/CD10- reactivity differentiates EMZBCL from other B-cell lymphomas.[40] Reactivity to CD5 would indicate a mantle cell lymphoma or small lymphocytic lymphoma whereas reactivity to CD10 is seen in Burkitt's lymphoma and follicular lymphoma. Cyclin D1 immunoreactivity distinguishes mantle cell lymphoma from EMZBCL (cyclin D1 -). The absence of BCL2 expression in follicles supports a diagnosis of EMZBCL over follicular lymphoma.[32] Ki-67 is helpful in distinguishing low- and high-grade lymphomas.[31] Co-expression of CD43 in B-cells and κ or λ light-chain restriction in plasma cells support a diagnosis of malignancy.[40] The expression of immunoglobulin M heavy chain by the plasma cells strongly supports a diagnosis of lymphoma.[39]

Table 3. Characteristic Immunohistochemical Profile of EMZBCL													
CD5	CD10	CD20	CD23	CD43	CD45	CD79α	Cyclin D1	BCL2	BCL6	MUM-1	PAX-5	EBV	Ki-67
-	-	+	V	V	-	+	-	+	-	+	+	-	L
V = variable H = high L = low													

Genetic abnormalities (Table 4) observed in EMZBCL of salivary glands include: t(1;14)(p22;q32), t(11;18)(q21;q21), t(14;18)(q32;q21), trisomy 3, trisomy 12, trisomy 18 and p16 deletion.[6, 30, 31] These acquired abnormalities induce the lymphoid tissue to transform into MALT lymphoma.[30] Trisomy 3 is the most common genetic abnormality in EMZBCL of salivary glands.[44] t(1;14)(p22;q32) results in the deregulation of the BCL10 gene, subsequent loss of its pro-apoptotic activity and acquisition of oncogenic potential by juxtaposing the immunoglobulin heavy-chain locus (IGH) located on 14q32 to the BCL10 region on locus 1p22.[31, 45] It presents in gastrointestinal (18%), pulmonary (7%) and salivary (2%) MALT lymphomas with an overall incidence rate of 1.6% among all sites.[1, 13, 16, 45] t(1;14)(p22;q32) has not been detected in skin, thyroid or ocular adnexa.[1] t(11;18)(q21;q21) results in the fusion of the apoptosis inhibitor-2 (API2) gene and the MALT lymphoma translocation (MALT1) gene to produce a functional API2-MALT1 fusion product.[1, 30, 31] It is highly specific for marginal zone MALT lymphomas[40] and has not been detected in nodal or splenic marginal zone lymphomas, or other NHL.[38, 40] t(11;18)(q21;q21) is the most common structural abnormality observed in EMZBCL of gastric (30%) and pulmonary (40%) MALT with an overall incidence of 17% among all sites.[1, 30, 45] It is rarely found in salivary glands, skin, ocular adnexa and thyroid with an incidence rate of 5%, 7%, 10% and 17%, respectively.[1, 6, 16, 31, 42, 46] When present, it

occurs as the sole genetic abnormality.[1, 30] t(14;18)(q32;q21) results in the juxtaposition of the immunoglobulin heavy chain locus (IGH) on 14q32 to the MALT1 gene region on locus 18q21, leading to the dysregulated expression of the oncogene MALT1.[30] When present, t(14;18)(q32;q21) occurs with additional genetic abnormalities such as trisomy 3.[30] This translocation has been observed in ocular adnexa/orbit (25%), skin (14%), salivary (16%) and pulmonary (10%) MALT lymphomas but not in gastric or thyroid MALT lymphomas.[1, 16, 30] It has an overall incidence of 11% among all sites.[45] t(3;14)(p14.1;q32) is observed in MALT lymphomas of the thyroid (50%), ocular adnexa/orbit (20%) and skin (10%) but there are no reported cases in the salivary glands, lung or gastrointestinal tract.[1, 16] It results in the juxtaposition of the immunoglobulin heavy chain locus (IGH) on 14q32 to the FOXP1 gene region on locus 3p14, deregulating the expression of the oncogene FOXP1.[13, 45] t(1;14)(p22;q32), t(11;18)(q21;q21) and t(14;18)(q32;q21) activate the necrosis factor (NF)-κB pathway which translocates NF-κB into the nucleus to activate certain genes important for cell activation, proliferation and survival.[31] These three translocations are mutually exclusive.[31, 46] Trisomy 18 shows a slight predilection for the salivary glands when compared to other sites.[45] It is not recognized if the presence or absence of the aforementioned genetic abnormalities in non-gastric EMZBCL has prognostic and/or therapeutic significance. At least in gastrointestinal cases, those exhibiting t(11;18)(q21;q21) tend to disseminate to regional lymph nodes and distant sites and fail to respond to antibiotic therapy for *Helicobacter pylori*.[43, 45] Therefore, it is more aggressive than gastric MALT lymphomas with other genetic abnormalities.

Remarkably, no consistent translocations have been identified in nodal marginal zone lymphoma.[13]

Table 4. Percentage of Genetic Abnormalities Encountered in EMZBCL According to Site of Occurrence							
Genetic aberration		**GI**	**Pulmonary**	**Salivary**	**Skin**	**Thyroid**	**Ocular**
t(1;14)(p22;q32)	BCL10/IGH	18	7	2	0	0	0
t(3;14)(p14.1;q32)	FOXP1/IGH	0	0	0	10	50	20
t(11;18)(q21;q21)	API2/MALT1	30	40	5	7	17	10
t(14;18)(q32;q21)	IGH/MALT1	0	10	16	14	0	25
GI = gastrointestinal							

EMZBCL responds to localized treatment, either surgical excision and/or radiation therapy, and does not tend to disseminate.[32] Partial or complete parotidectomy is performed when present in the parotid gland. Complete removal of the submandibular or sublingual gland is recommended when involved by disease. Recurrences (25-35% from all sites) can be observed many years after initial presentation, which may include other extranodal sites.[43] A higher incidence of recurrence is seen in extragastric MALT lymphomas (24-40%) when compared to primary gastric disease (5-20%), especially those cases with t(11;18)(q21;q21).[16, 43, 45] The overall prognosis of EMZBCL is favorable, especially since EMZBCL exhibits a slow evolution and remains localized to its site of origin for long periods of time. When involvement of salivary gland lymph nodes is documented, the prognosis is similar to primary nodal MALT lymphoma.[32] The 5-year survival rate for all MALT lymphoma cases is estimated at 85-95%.[43]

II. MATERIALS AND METHODS

Samples: A search utilizing the Joint Pathology Information Management System (JPIMS) at the Joint Pathology Center (JPC) for cases diagnosed as "extranodal marginal zone B-cell lymphoma (EMZBCL)" in major salivary glands (parotid, submandibular, sublingual) from 31 December 1991 until 31 October 2014 was conducted. Only nineteen cases of formalin-fixed, paraffin-embedded specimens and corresponding hematoxylin and eosin (H&E) stained slides were identified in the database meeting the inclusion criteria. The available nineteen cases were retrieved from the Joint Pathology Center Tissue Repository located at the JPC, Forest Glen Annex, Silver Spring, Maryland. An identification number was assigned to each of the retrieved specimens randomly (1 through 19) to protect personally identifiable information. All the retrieved cases were recorded in a master list documenting the JPIMS accession numbers and the corresponding assigned identification numbers. The master list was kept separate from the study samples during the length of the study. The retrieved cases were reviewed with two oral and maxillofacial pathologists from the JPC to verify the diagnoses using today's diagnosis criteria and to determine that sufficient paraffin-embedded tissue was available for further immunohistochemical (IHC) and molecular studies. Two of the specimens were excluded from the study due to lack of sufficient remaining tissue for further testing. When available, the demographic (age, sex, gender, ethnicity) and medical (medications, medical history, tissue site) information was recorded in the master data collection sheet (Table 5).

Table 5. Data Collection			
Specimen assigned #_____			
Age		Gender:	Ethnicity:
Medications			
Medical History			
Tissue Site			
Part I: Immunohistochemistry for Characterization			
	Present	Absent	Comments (indicate if undetermined here)
CD5			
CD10			
CD20			
CD23			
CD43			
CD79a			
Cyclin D1			
BCL2			
Part II: Light-Chain Restriction			
	Present (%)	Absent	Comments (indicate if undetermined here)
Kappa			
Lambda			
Part III: Ig Heavy Chain Rearrangement			
Circle one: Monoclonal Polyclonal Undetermined Comments:			
Part IV: FISH studies			
MALT1 break apart probe Circle one: Observed Not observed Undetermined Comments:			
Chromosome 3 copy number increased Circle one: Observed Not observed Undetermined Comments:			
Chromosome 18 copy number increased Circle one: Observed Not observed Undetermined Comments:			

Immunohistochemistry: Missing immunohistochemical (IHC) stains needed to characterize tissue samples as EMZBCL were performed when necessary (Table 6). IHC studies were conducted utilizing a Roche Ventana Benchmark Ultra automated slide-stainer. Formalin-fixed, paraffin-embedded tissue samples were sectioned at 4

micrometers (µm) and applied to positive-charged slides. The slides were deparaffinized in xylene, rehydrated in 100%, 95% and 80% ethanol sequentially and equilibrated in 7.6 pH tris-based buffer. Finally, the slides were heated to 37ºC, incubated with pre-diluted antibody, and counterstained with hematoxylin with subsequent application of bluing reagent.

Table 6. Immunohistochemical Antibody Panel for Characterization of EMZBCL

Antibody	Clone[(a)]	Antigen retrieval[(b)]	Incubation time (minutes)
CD5	SP19 monoclonal	water bath	48
CD10	56C6 monoclonal	water bath	32
CD20	L26 monoclonal	water bath	32
CD23	SP23 monoclonal	water bath	32
CD43	L60 monoclonal	water bath	32
CD79α	SP18 monoclonal	water bath	32
Cyclin D-1	SP4-R monoclonal	water bath	32
BCL2	124 monoclonal	water bath	32
Kappa (κ)	polyclonal	water bath	32
Lambda (λ)	polyclonal	water bath	32

(a) The source of all clones was Ventana (Ventana Medical Systems, Tucson AZ).
(b) Slides heated at 95ºC in tris-based buffer (Ventana cell conditioning solution CC1) for 8 minutes

Immunoglobulin heavy chain (IgH) gene rearrangement: Polymerase chain reaction (PCR) was used to increase the amount of DNA available to conduct the IgH gene rearrangement studies. Formalin-fixed, paraffin-embedded tissue was used for PCR following the methodology described by Reed (1993).[47] Two 7-8 µm paraffin sections from each block were deparaffinized in xylene, rehydrated with ethanol, and dried. Samples were then digested with Proteinase K at 55ºC for 1 hour, followed by heating to 95ºC for 10 minutes. The samples were centrifuged and placed into a thermal cycler using approximately 1 U Taq polymerase, 100 nM of each primer (see Table 7), 200 µM dNTPs, 1.5 mM MgCl2, 50 mM KCl, 10 mM tris-HCl, and .01% gelatin. Appropriate

controls were used with each run. The semi-nested PCR protocol described by Wan (1990)[48] was performed as described below.

Table 7. Primers Used for the Polymerase Chain Reaction[47, 48]	
Primer	**Sequence**
V region (FR3A)	5-ACA-CGG-C(C/T)(G/C)-TGT-ATT-ACT-GT-3'
J Region (CFW1; outer nest)	5'-ACC-TGA-GGA-GAC-GGT-GAC-CAG-GGT-3'
J Region (VLJH; inner nest)	5'-GTG-ACC-AGG-GT(A/G/C/T)-CCT-TGG-CCC-CAG-3'

For the initial amplification, primers FR3A and CFW1 were used. The primers were denatured at 94ºC for 5 minutes. Forty cycles of 1-minute denaturation at 94ºC, 1-minute annealing at 55ºC and 1-minute chain extension at 72ºC were performed. The cycles concluded with 7 minutes of chain elongation at 72ºC. Subsequently, 10µl of a 1:1,000 dilution from each tube was transferred to a new tube with fresh reagents, including fluorescent tags ([α-^{32}P]dATP) and primers FR3A and VLJH. Five minutes of denaturation at 94ºC followed by 20 cycles of 1-minute denaturation at 94ºC, 1-minute annealing at 55ºC and 1-minute chain extension at 72ºC were completed. The cycles concluded with 7 minutes of chain elongation at 72ºC. With this semi-nested PCR protocol, one of the primers used in the second set of cycles was allowed to hybridize to a sequence within the corresponding primer in the first set of cycles to prevent non-specific amplification products from the first set of cycles ("outer nest") in the second set of cycles ("inner nest").[47] Amplified products were separated by capillary electrophoresis utilizing an ABI 3100 (Applied Biosystems, Foster City, CA). Samples were injected into thin, fused-silica capillaries previously filled with polymer. A voltage was applied causing the DNA fragments to migrate towards the positive (+) end of the capillaries. Shorter DNA fragments moved faster than longer DNA fragments. As the

DNA fragments passed through the excitation beam, they fluoresce. An optical device captured the information which was then transferred to a computer workstation for processing.

Fluorescence in situ hybridization: The Vysis LSI ® MALT1 Break Apart FISH Probe Kit (Abbott Molecular, Downer Grove, IL) was used to identify translocations involving the rearrangement of chromosome locus 18q21.31 (MALT1 gene) (Figure 1). Manufacturer's instructions were followed with minor modifications.

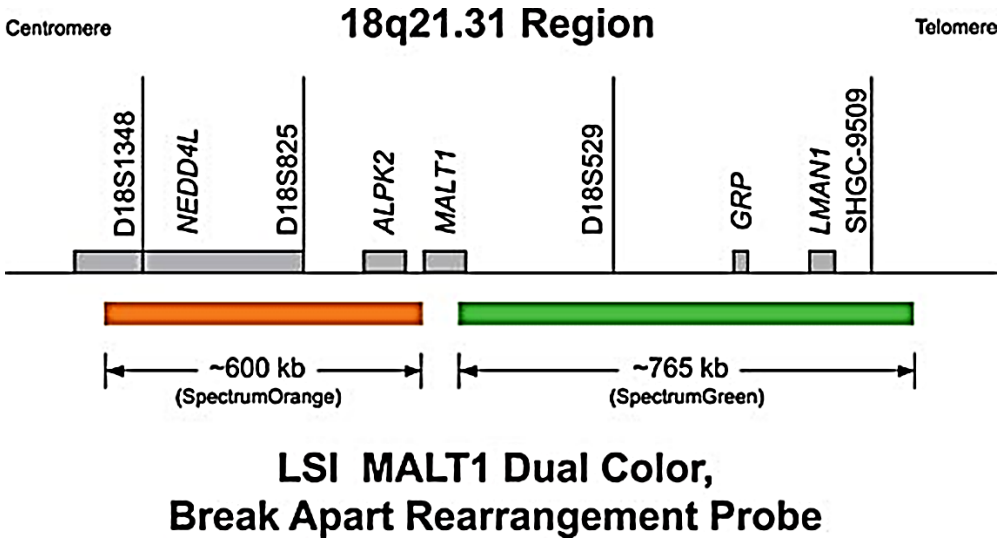

Figure 1. Vysis LSI MALT1 break apart probe used to screen for the presence of translocations involving chromosome 18 in the q21.31 region, MALT1 gene. "Vysis LSI MALT1 Dual Color Break Apart Rearrangement Probe." Abbott Molecular, n.d. Web. <https://www.abbottmolecular.com/us/chromosome/18.html> accessed 20February2015.

Four µm formalin fixed, paraffin embedded sections were incubated for 24 hours at 56°C in an oven and then deparaffinized three times in Hemo De® (xylene-alternative solvent) for five minutes each time. The sections were dehydrated twice in 100% ethanol for 3 minutes each time and, subsequently, in 95% alcohol for 3 minutes. They

were then immersed in a HCl 0.2N pre-treatment solution (pre-heated in a 97°C water bath) for 25 minutes. After washing with deionized water (dH_2O), the slides were immersed in protease solution (60mg/ml pepsin into 59.4ml of pre-heated protease buffer at 37ºC) and incubated for 45 minutes in a 37ºC water bath to facilitate DNA access for the probes. The slides were then immersed in wash buffer for 5 minutes, briefly rinsed in dH_2O, and dried for 5 minutes. Approximately 10 µl of probe mix (7 µl locus-specific identifier (LSI) buffer, 1 µl LSI DNA probe, 2 µl purified water) was applied to each specimen, coverslipped and sealed with rubber cement. One probe was labeled with SpectrumOrange, specific for ALPK2 [~600 kb]. The second probe was labeled with SpectrumGreen, specific for MALT1 [~765 kb]. The slides were incubated in a Thermobrite Statspin® (Abbott Molecular, Downer Grove, IL) slide incubator for 6 minutes at 75ºC and then for 24 hours at 37ºC to automate the denaturation and hybridization steps.

After the rubber cement was removed, the slides were placed in post-hybridization buffer I at room temperature in the dark to soak off the coverslips. The slides were then placed in Coplin jars containing post hybridization buffer I (pre-heated in a water bath at 75°C) for 5 minutes. Afterwards, the slides were washed in post-hybridization buffer II for 30 seconds at room temperature, briefly rinsed in dH_2O, dried for 5 minutes, counterstained with 10 µl DAPI (4',6-diamidino-2-phenylindole) blue fluorescent stain and coverslipped. Subsequently, the slides were placed in a -20°C freezer for at least 30 minutes prior to reviewing them using Cytogenetics Suite (Bioview Ltd.) software and a fluorescent microscope. This procedure was repeated twice more

using chromosome enumeration probes (CEP) targeted at the centromeres of chromosome 3 and chromosome 18 (Vysis CEP3 (D3Z1), CEP3, 3p11.1-q11.1 Alpha Satellite DNA; Vysis CEP18 (D18Z1), 18p11.1-q11.1 Alpha Satellite DNA both in SpectrumOrange) (Figure 2).

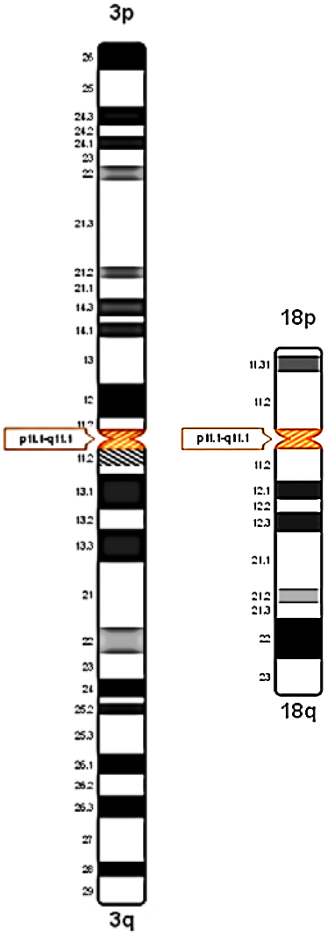

Figure 2. Vysis CEP probes targeting the centromeres of chromosome 3 and chromosome 18. "Vysis CEP Probes." Abbott Molecular, n.d. Web. <https://www.abbottmolecular.com/us/chromosome/3.html>, <https://www.abbottmolecular.com/us/chromosome/18.html> accessed 20February2015.

Cases exhibiting translocations involving chromosome 18 at MALT1 break apart region were further tested for t(11;18)(q21;q21) and t(14;18)(q32;q21) using the described FISH methodology with Vysis LSI t(11;18)(q21;q21)/API2-MALT1kit (Figures 3 and 4) and Vysis LSI t(14;18)(q32;q21)/IGH-MALT1kit containing dual-color dual-fusion DNA probes (Abbott Molecular, Downer Grove, IL) (Figures 4 and 5).

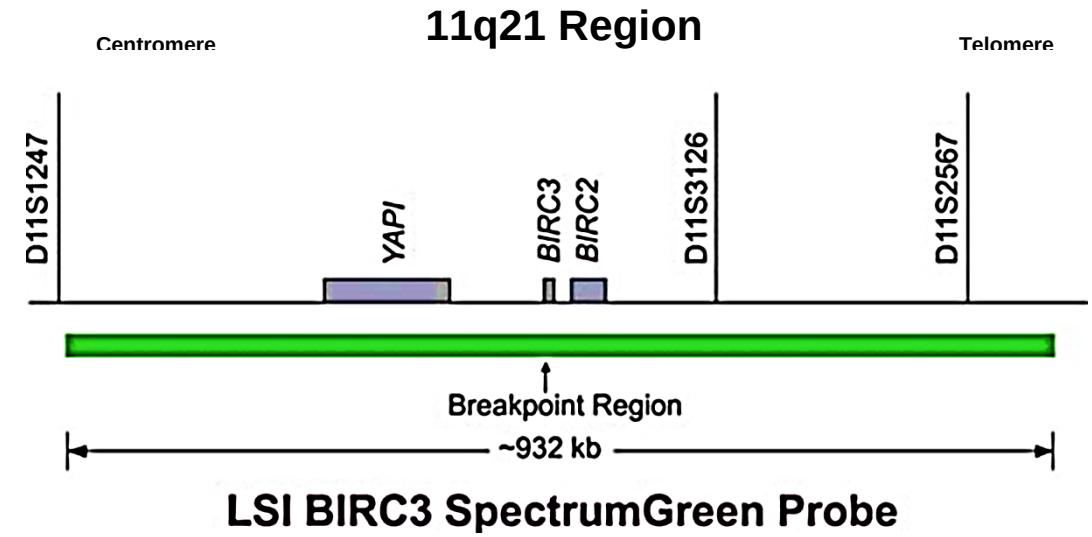

Figure 3. Vysis LSI API2 (also known as BIRC3) probe used to detect the presence of translocations involving chromosome 11 in the q21 region, API2 gene. "Vysis LSI API2 SpectrumGreen." Abbott Molecular, n.d. Web <https://www.abbottmolecular.com/us/chromosome/11.html> accessed 20February2015.

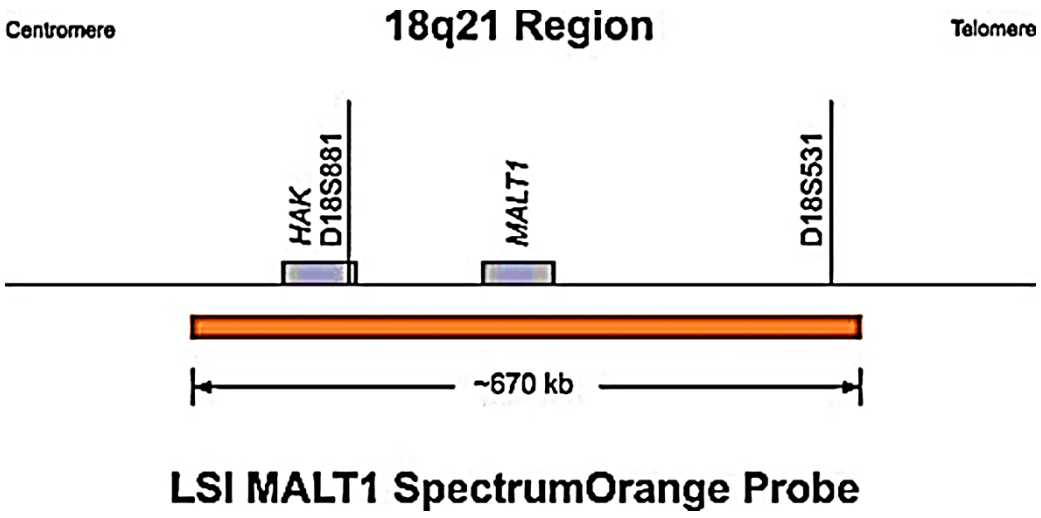

Figure 4. Vysis LSI MALT1 probe used to detect the presence of translocations involving chromosome 18 in the q21 region, MALT1 gene. "Vysis LSI MALT1 SpectrumOrange Probe." Abbott Molecular, n.d. Web. <https://www.abbottmolecular.com/us/chromosome/18.html> accessed 20February2015.

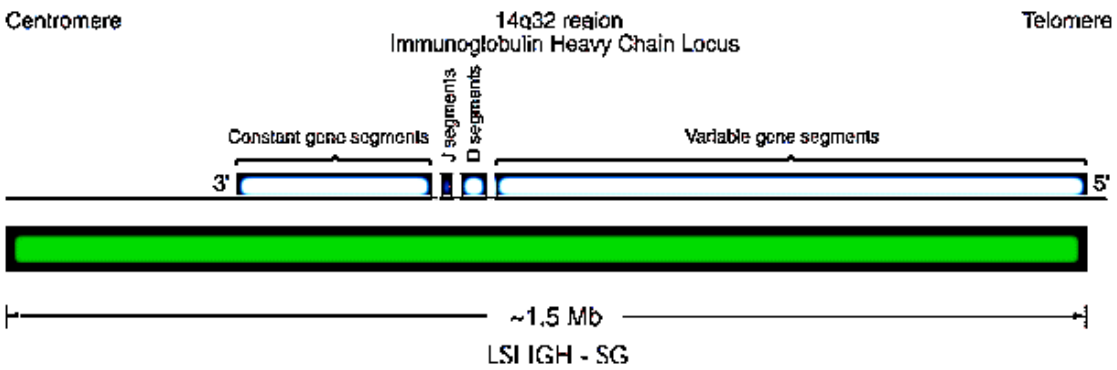

Figure 5. Vysis LSI IGH probe used to detect the presence of translocations involving chromosome 14 in the q32 region, IGH gene. "Vysis LSI IGH SpectrumGreen Probe." Abbott Molecular, n.d. Web. <https://www.abbottmolecular.com/us/chromosome/14.html> accessed 20February2015.

III. RESULTS

Demographics: The patient population was comprised of nine females ages 40 to 80 years old (53%) and eight males ages 47 to 83 years old (47%). The mean age of the cohort was 60 years old and the median age was 53 years old. One female patient was Caucasian. The remaining patients did not disclose their ethnic background. Three female patients ages 66, 65 and 84 suffered from Sjögren syndrome, a synchronous maltoma of the palate and increased rheumatoid factor, respectively. One seventy-eight year old male patient reported an enlarged prostate. The medical history was unknown for the other thirteen patients. The extranodal marginal zone B-cell lymphoma (EMZBCL) appeared in the parotid gland in fifteen patients (88%) and in the submandibular gland in 2 female patients (12%). Table 8, Figure 6 and Figure 7 summarize patient demographics.

Table 8. Patient Demographics					
Specimen number	**Age**	**Gender**	**Ethnicity**	**Medical History**	**Location (gland)**
2a	52	M	unknown	unknown	L parotid
3a	62	M	unknown	unknown	R parotid
4a	48	F	Caucasian	unknown	R parotid
5a	79	M	unknown	unknown	R parotid
6a	66	F	unknown	Sjögren syndrome	L parotid
7a	52	M	unknown	unknown	L parotid
8a	65	F	unknown	Synchronous maltoma*	L parotid
10a	47	M	unknown	unknown	R parotid
11a	40	F	unknown	unknown	L submandibular
12a	42	F	unknown	unknown	L parotid
13a	79	M	unknown	unknown	R parotid
14a	82	F	unknown	RH increased	L parotid
15a	83	M	unknown	unknown	L parotid
16a	47	F	unknown	unknown	R submandibular
17a	78	M	unknown	enlarged prostate	R parotid
18a	50	F	unknown	unknown	L parotid
19a	53	F	unknown	unknown	L parotid
L= left R= right *palate RH= rheumatoid factor					

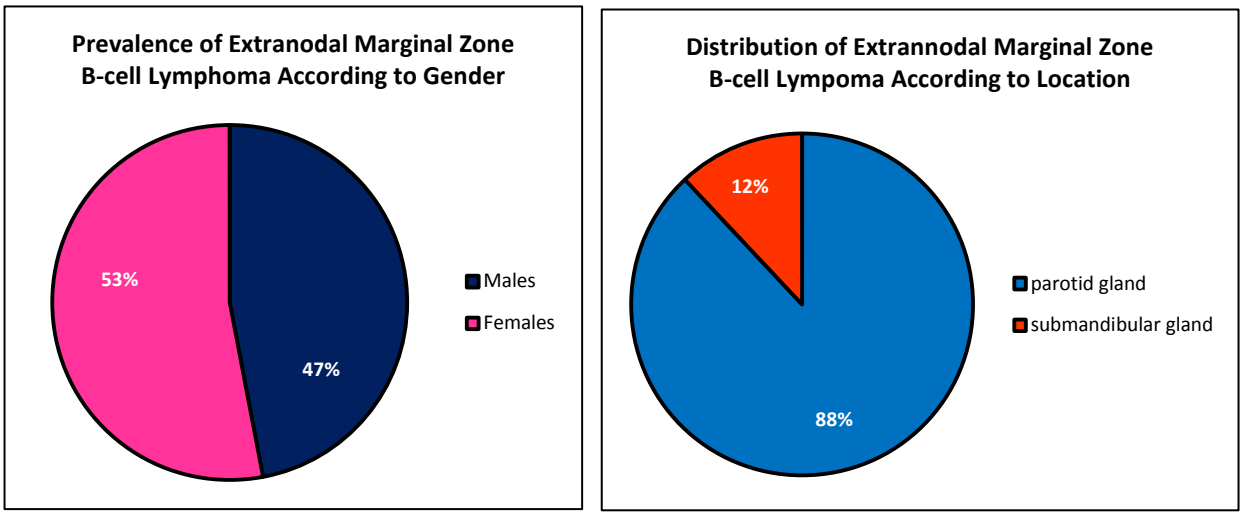

Figure 6. Prevalence of EMZBCL according to gender and location.

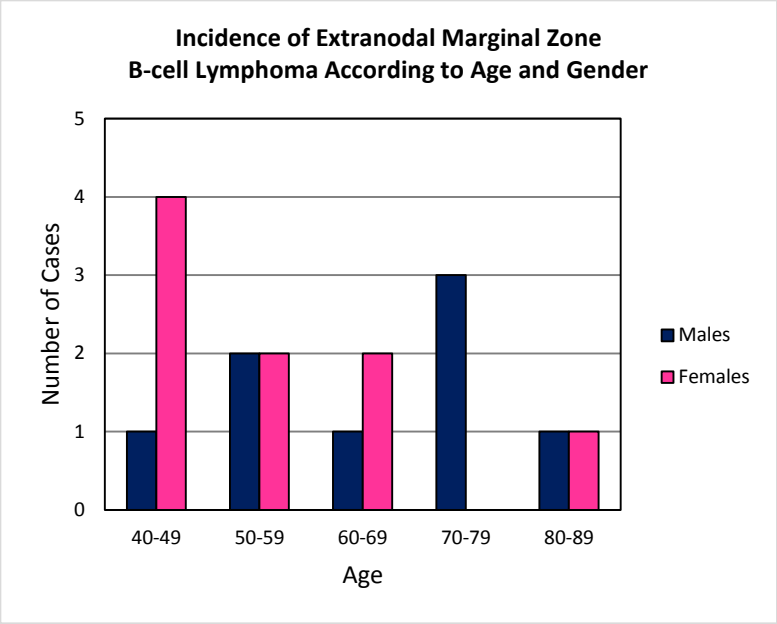

Figure 7. Incidence of Extranodal Marginal Zone B-cell Lymphoma According to Age and Gender.

Histopathologic features: The salivary gland parenchyma was expanded in fourteen cases (82%) with preservation of the lobular architecture. Only twelve cases (71%) had residual gland parenchyma such as salivary ducts and scattered cells at the periphery. Sixteen cases (94%) exhibited effacement of the glandular parenchyma by epitheliotrophic lymphoid tissue (Figure 8). All samples demonstrated LELs, around which coalescing halos of monocytoid B-cells were identified (Figure 9A, B). The LELs were infiltrated by the neoplastic monocytoid B-cells (Figure 9C). Germinal centers were identified in all samples, with eleven (65%) samples exhibiting atrophic germinal centers and eight samples (47%) revealing serpiginous pattern.

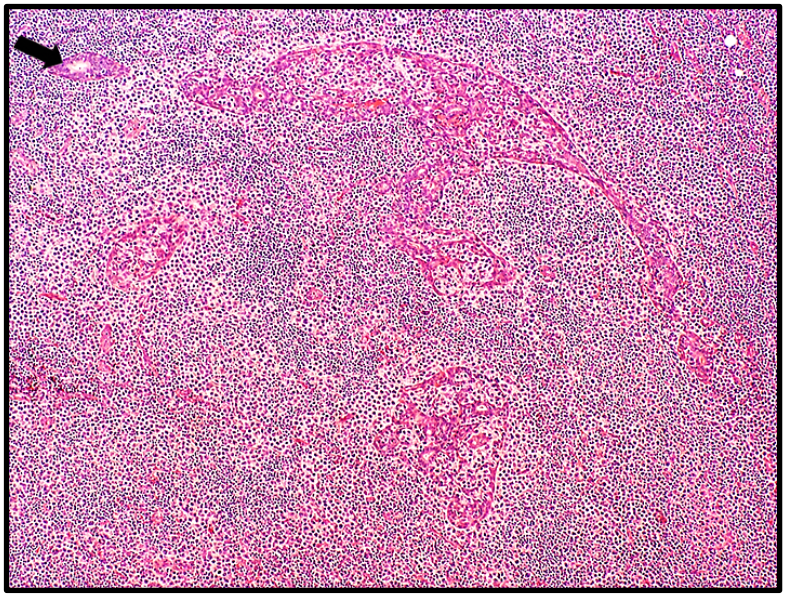

Figure 8. Effacement of the salivary gland parenchyma by epitheliotrophic lymphoid tissue. Limited residual gland parenchyma is noted (arrow). Hematoxylin and eosin (H&E) stain x40.

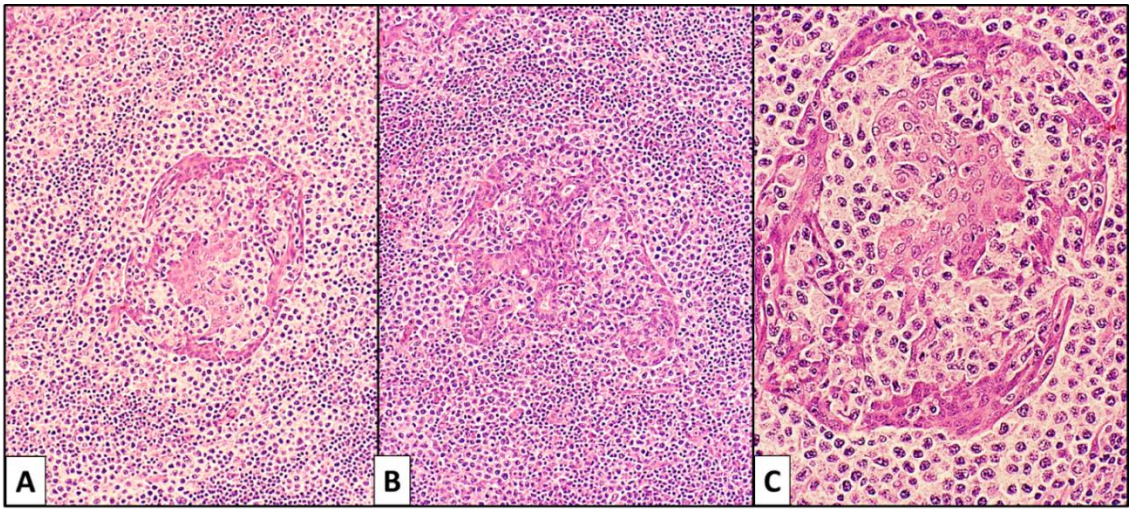

Figure 9. (A, B) Lymphoepithelial lesions with a halo of coalescing monocytoid B-cells around them. H&E stain x100. (C) Destruction and infiltration of the lymphoepithelial lesion by neoplastic monocytoid B-cells. H&E stain x200.

Immunohistochemical (IHC) studies: Kermix (AE1/AE3/CK1) highlighted the LELs in all cases (Figure 10). All seventeen samples were positive for CD20, CD79α and BCL2 (Figures 11 and 12). BCL2 immunoreactivity was not observed in the germinal centers but in the interfollicular spaces (Figure 12). CD5 highlighted only the background

interfollicular T-cells in all but one specimen (94%) (Figure 12). CD10 was positive only in the germinal centers of eleven samples (65%) (Figure 12). Six cases (35%) did not show any CD10 positivity. CD23 exhibited immunoreactivity in the germinal centers of 16 specimens (94%) (Figure 11). Cyclin D1 failed to immunoreact in all cases (Figure 12). The neoplastic cells were negative for CD5, CD10 and CD23 in 100% of the specimens (Figures 11 and 12). CD43 was positive in the neoplastic B-cells in five specimens (29%), equivocal in one specimen (6%) and negative in the other eleven cases (65%). Ten cases (59%) were kappa (κ) light-chain restricted. The remainder seven cases (41%) were inconclusive for light-chain restriction, either κ or lambda (λ). No λ light-chain restriction was observed. The results for those cases exhibiting κ light-chain restriction were confirmed with previously performed in situ hybridization (ISH) studies for κ and λ (Figure 13). Table 9 summarizes IHC results.

Table 9. IHC Characterization

Specimen	CD5[#]	CD10[*]	CD20	CD23[*]	CD43	CD79α	Cyclin D1	BCL2[$]	κ	λ
2a	-	+	+	+	-	+	-	+	+	-
3a	-	+	+	+	-	+	-	+	+	-
4a	-	+	+	+	-	+	-	+	+	-
5a	-	-	+	-	-	+	-	+	I	-
6a	-	-	+	+	-	+	-	+	+	-
7a	-	+	+	+	-	+	-	+	+	-
8a	-	+	+	+	+	+	-	+	+	-
10a	-	-	+	+	+	+	-	+	+	-
11a	-	+	+	+	+	+	-	+	+	-
12a	-	+	+	+	I	+	-	+	I	-
13a	-	No GC	+	+	-	+	-	+	I	-
14a	-	+	+	+	-	+	-	+	+	-
15a	-	+	+	+	-	+	-	+	+	-
16a	-	-	+	+	-	+	-	+	I	-
17a	-	-	+	+	-	+	-	+	I	-
18a	-	+	+	+	+	+	-	+	I	-
19a	-	+	+	+	+	+	-	+	I	-

κ = kappa light-chain restriction
λ = lambda light-chain restriction
GC = germinal center
I = indeterminate
+ = positive immunoreactivity
- = failed to immunoreact
= highlighted interfollicular T-cells only
* = germinal center only; negative in neoplastic cells
$ = not in germinal centers

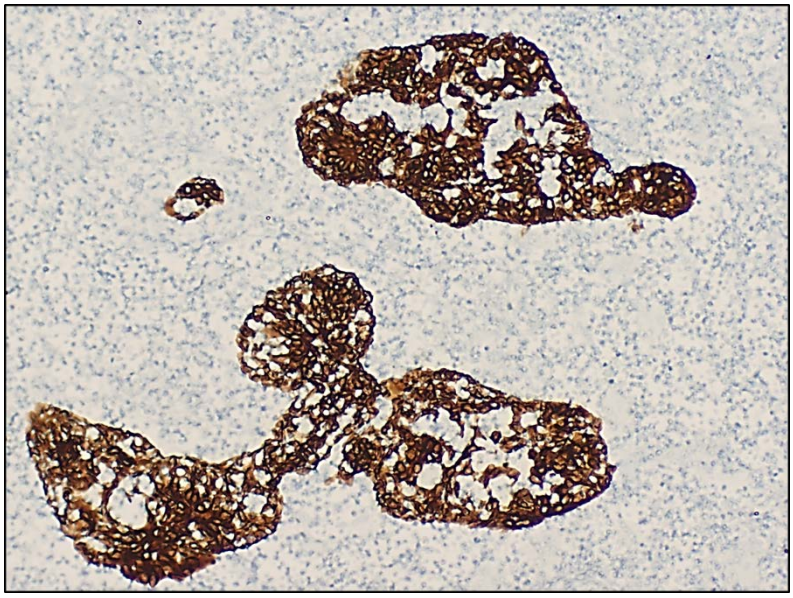

Figure 10. LELs highlighted with Kermix (AE1/AE3/CK1). x100.

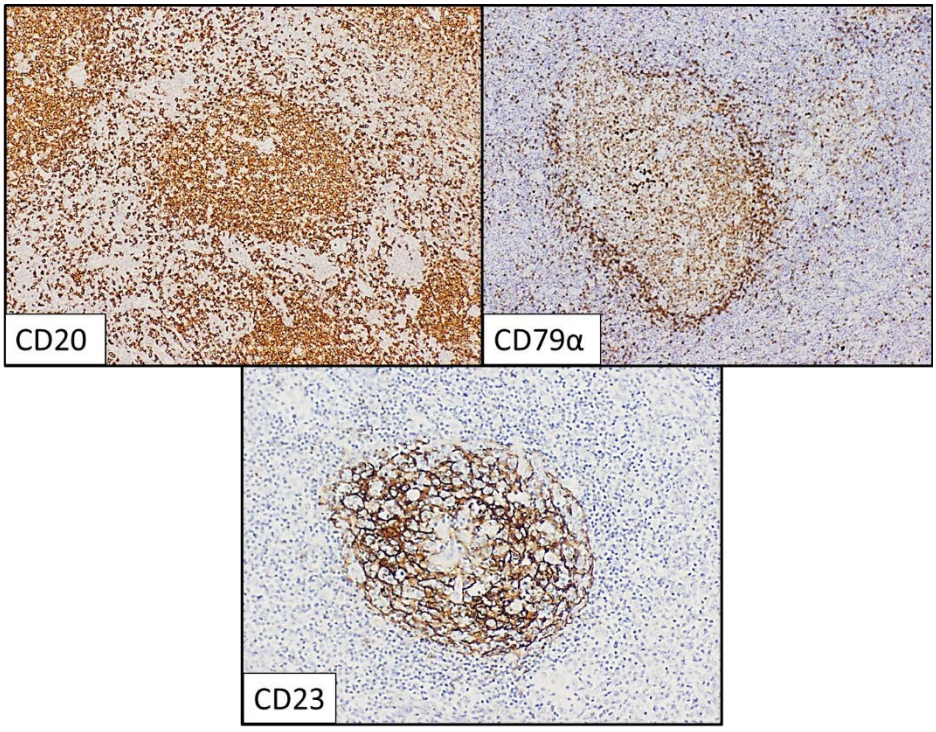

Figure 11. Immunoreactivity for CD20 and CD79α confirms a B-cell immunophenotype. CD23 highlights the dendritic mesh network within the germinal centers. x40.

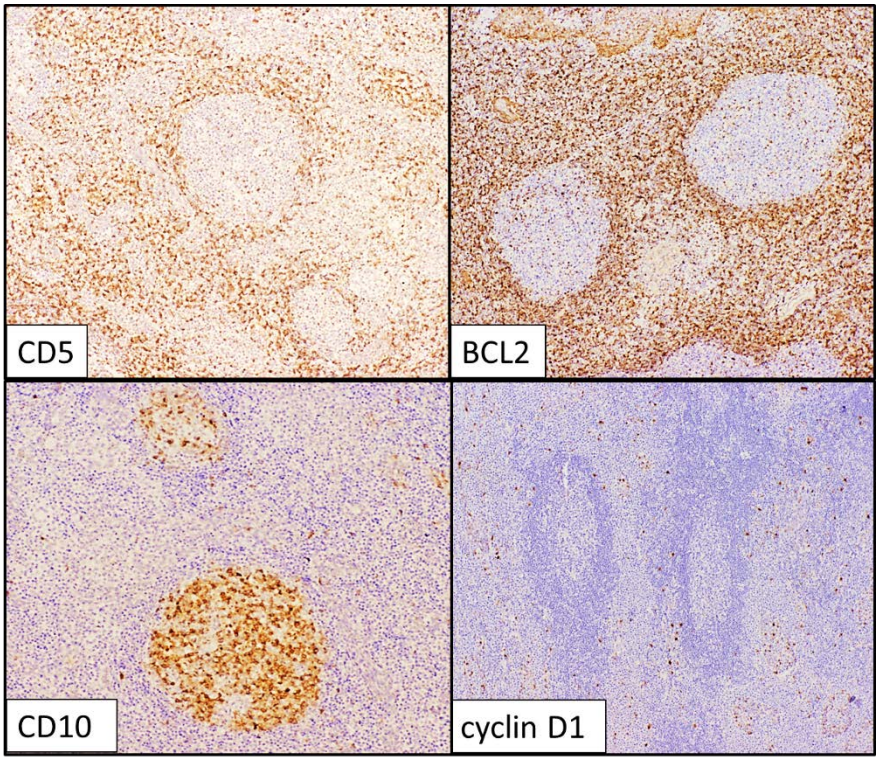

Figure 12. CD5 highlights background interfollicular cells only. CD10 highlights the germinal centers only. CD5 and CD10 fail to immunoreact with the neoplastic monocytoid B-cells. Cyclin D1 is negative. BCL2 does not immunoreact in the germinal centers. x40.

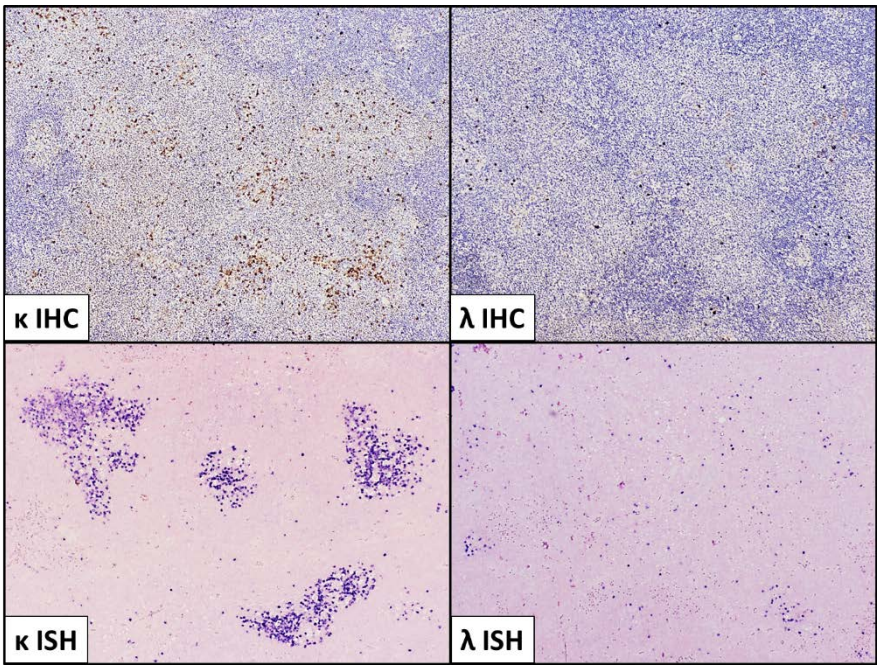

Figure 13. κ light-chain restriction was demonstrated by IHC and ISH. λ light-chain restriction was not observed. This profile confirms monoclonality. x40.

Immunoglobulin heavy chain (IgH) gene rearrangement: Fifteen cases (88%) were monoclonal while two cases (12%) were polyclonal. The two cases with rearrangement of the MALT1 gene were monoclonal (13%). Four of the monoclonal samples (27%) did not exhibit any other genetic abnormalities. Increased copy number of both, chromosome 3 and chromosome 18, was observed in four monoclonal cases (27%) which failed to show rearrangement of the MALT1 gene. Three of the monoclonal specimens (20%) demonstrated an increased copy number of chromosome 3 but no rearrangement of the MALT1 gene nor increased copy number of chromosome 18. The remaining two monoclonal cases (13%) exhibited increased copy number of chromosome 18 but no rearrangement of the MALT1 gene nor increased copy number of chromosome 3. One of the polyclonal specimens exhibited increased copy number of chromosome 3 and chromosome 18. The other polyclonal specimen demonstrated increased copy number of chromosome 3 only. None of the polyclonal cases demonstrated MALT1 gene rearrangement. Results are summarized in Table 10.

Fluorescence in situ hybridization (FISH): Only two cases (12%) demonstrated rearrangement of the MALT1 gene in chromosome 18q21 (Figure 14). One of these cases also exhibited increased copy number of chromosome 3 while the other case did not reveal any additional abnormalities. Both cases were located in the parotid gland.

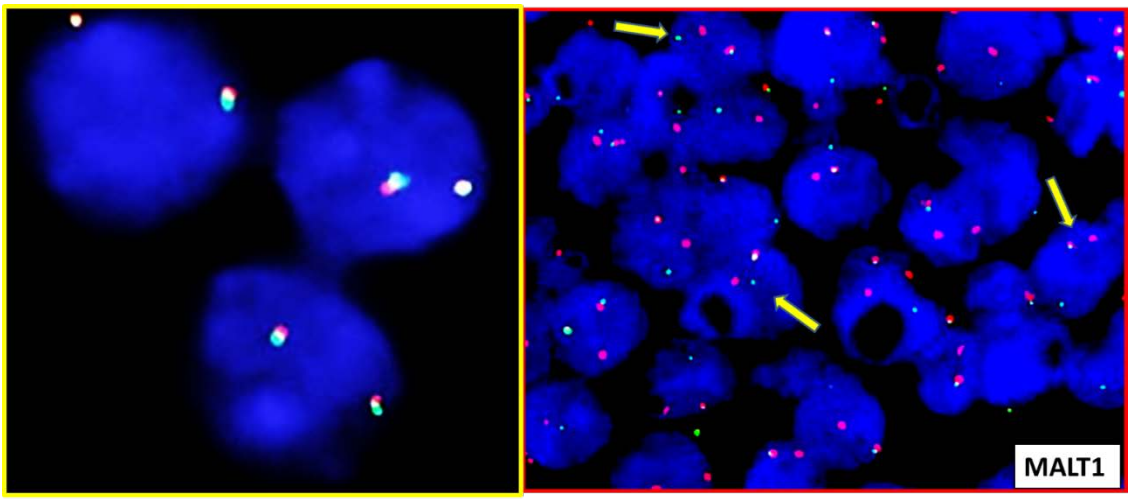

Figure 14. Hybridization of the Vysis LSI MALT1 Dual Color Break Apart Rearrangement Probe. **Left:** Interphase cells lacking t(18q21) in the MALT1 gene region. A two fusion signal pattern reflects the two intact copies of MALT1. From *https://www.abbottmolecular.com/us/chromosome/18.html*. **Right:** Cells exhibiting MALT1 break apart probe (case 18) (yellow arrows). The one fusion, one orange and one green signal pattern indicates rearrangement of one copy of the MALT1 gene region, observed in t(18q21). *Courtesy of Dr. Rachel Werner.*

Ten cases (59%) demonstrated increased copy number for chromosome 3, eight in the parotid gland (47%) and two in the submandibular gland (12%) (Figure 15). Four of these cases (40%), three in the parotid gland and one in the submandibular gland, exhibited no other abnormalities. Five of the ten cases (50%), four in the parotid gland and one in the submandibular gland, also displayed increased copy number of chromosome 18. One case (10%) revealed rearrangement of the MALT1 gene, located in the parotid gland.

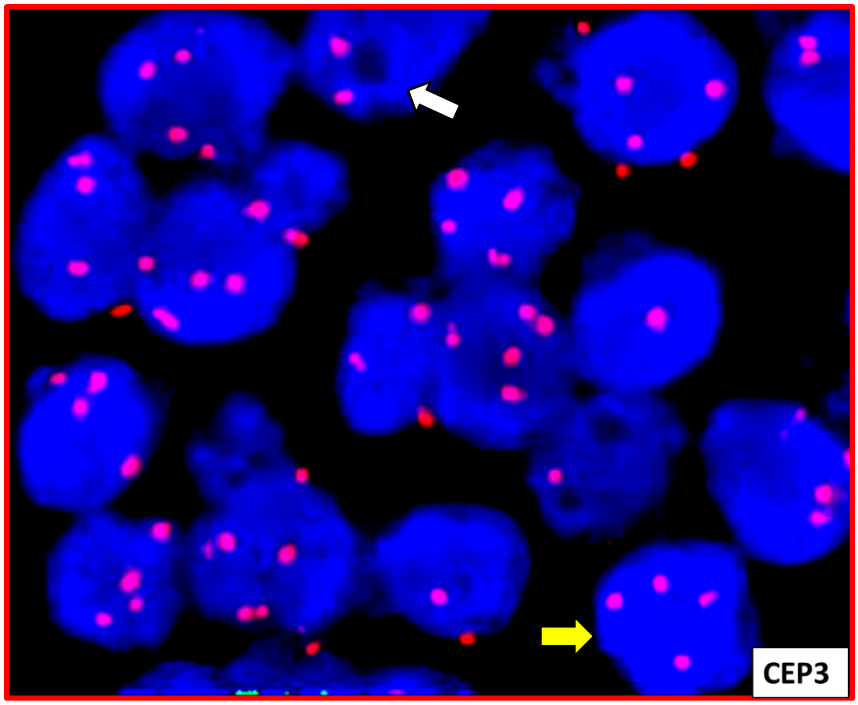

Figure 15. Vysis CEP3 probe. Cells demonstrate increased copy number of chromosome 3 by exhibiting more than two signals per cell (case 13) (yellow arrow). Cells with only two orange signals do not have increased chromosome number (white arrow). *Courtesy of Dr. Rachel Werner.*

Seven specimens (41%), six in the parotid gland (35%) and one in the submandibular gland (6%), demonstrated increased copy number of chromosome 18 (Figure 16). Two of these specimens located in the parotid gland (29%) showed no other abnormalities. Five of the seven specimens (71%), four in the parotid gland and one in the submandibular gland, also exhibited an increased copy number of chromosome 3. The two female patients with a medical history of autoimmune disease (SS and increased rheumatoid factor) demonstrated increased copy number of chromosome 18 in the parotid EMZBCL. In 30% of the cases, four in the parotid gland and one in the submandibular gland, increased copy number of chromosome 3 occurred concurrently with increased copy number of chromosome 18 (Figure 18). None of the

cases that exhibited increased copy number of chromosome 18 showed rearrangement of the MALT1 gene.

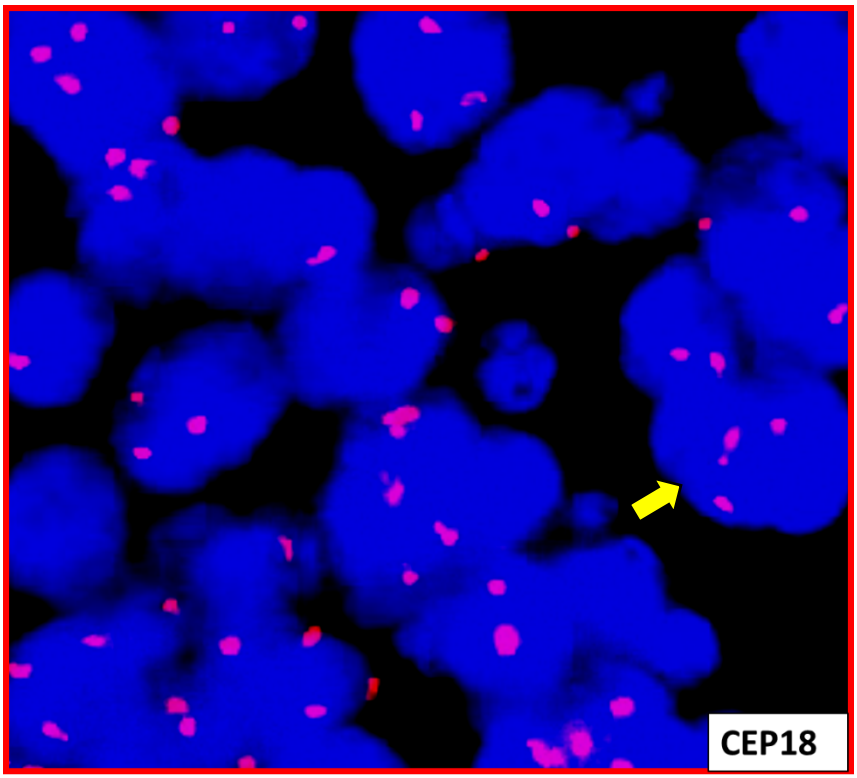

Figure 16. Vysis CEP18 probe. Cells demonstrate increased copy number of chromosome 18 by exhibiting more than two signals per cell (case 4) (yellow arrow). Cells with only two orange signals do not have increased chromosome number (white arrow). *Courtesy of Dr. Rachel Werner.*

The two cases that demonstrated rearrangement of the MALT1 gene were subjected to further testing for API2/MALT1 and IGH/MALT1 gene rearrangements, which probe for the reciprocal translocations t(11;18)(q21;q21) and t(14;18)(q32;q21) respectively. Both cases failed to show API2/MALT1 gene rearrangement [t(11;18)(q21;q21)]. One case exhibited IGH/MALT1 gene rearrangement [t(14;18)(q32;q21)] while demonstrating increased copy number of chromosome 3 but no increased copy number of chromosome 18 (Figure 17). Twenty-four percent of our

cases exhibited no genetic abnormalities. Table 10 and Figure18 summarize FISH results.

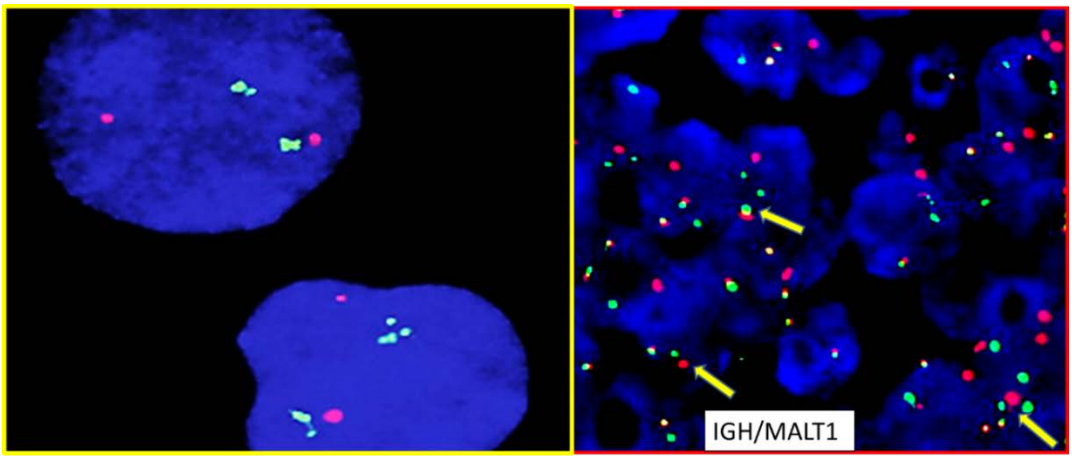

Figure 17. Hybridization of the Vysis LSI IGH/MALT1 t(14;18)(q32;q21) Dual Color, Dual Fusion Translocation Probe. **Left:** Interphase cells lacking IGH/MALT1 gene rearrangement, t(14;18)(q32;q21). From *https://www.abbottmolecular.com/us/chromosome/18.html*. **Right:** Cells exhibiting IGH/MALT1 gene rearrangement (case 18) (yellow arrows). The one orange, one green and two fusion signal pattern indicates t(14;18)(q32;q21) presence. *Courtesy of Dr. Rachel Werner.*

Table 10. IgH and FISH Results

Specimen	IgH*	MALT1 gene rearrangement	CEP3	CEP18	API2/MALT1# rearrangement	IGH/MALT1$ rearrangement
2a	M	present	normal	normal	absent	absent
3a	M	absent	normal	normal	N/A	N/A
4a	M	absent	normal	increased	N/A	N/A
5a	M	absent	normal	normal	N/A	N/A
6a	M	absent	normal	increased	N/A	N/A
7a	P	absent	increased	normal	N/A	N/A
8a	M	absent	normal	normal	N/A	N/A
10a	M	absent	normal	normal	N/A	N/A
11a	M	absent	increased	increased	N/A	N/A
12a	M	absent	increased	normal	N/A	N/A
13a	M	absent	increased	increased	N/A	N/A
14a	M	absent	increased	increased	N/A	N/A
15a	P	absent	increased	increased	N/A	N/A
16a	M	absent	increased	normal	N/A	N/A
17a	M	absent	increased	normal	N/A	N/A
18a	M	present	increased	normal	absent	present
19a	M	absent	increased	increased	N/A	N/A

CEP3: increased copy number chromosome 3
CEP18: increased copy number chromosome 18
*IgH = Immunoglobulin heavy chain (M = monoclonal; P = polyclonal)
# t(11;18)(q21;q21)
$ t(14;18)(q32;q21)
N/A: not tested

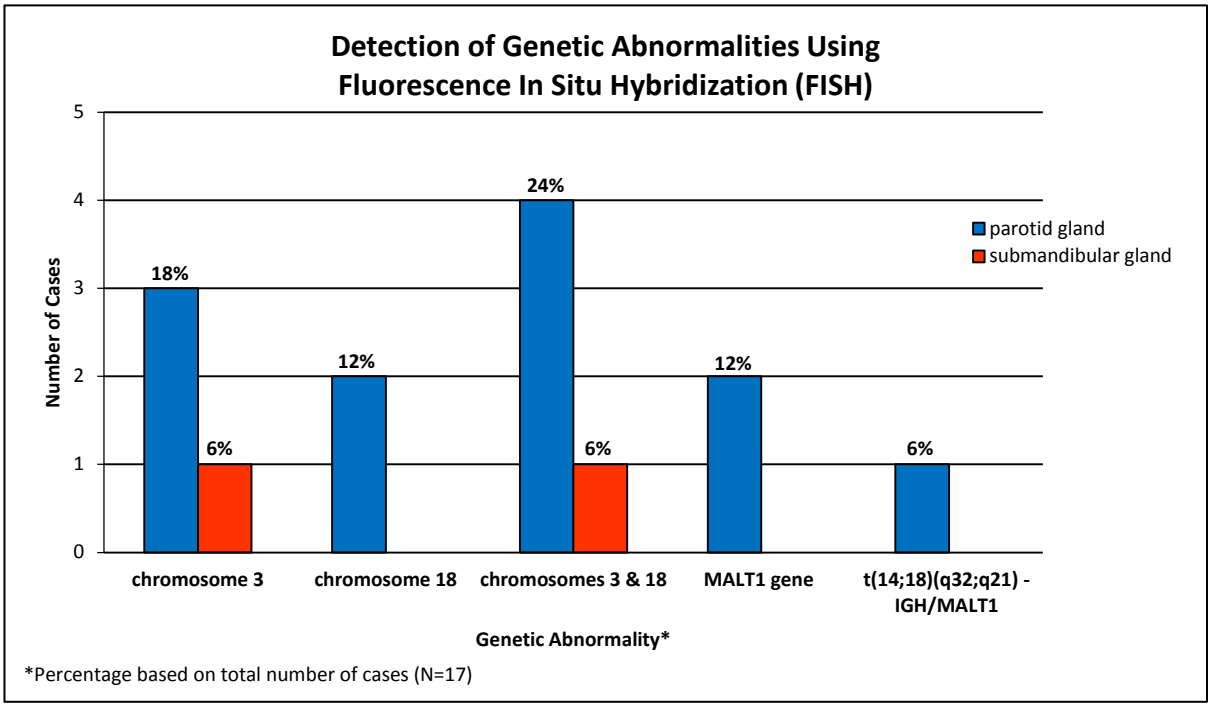

Figure 18. Incidence of genetic abnormalities detected by FISH according to location.

IV. DISCUSSION

Sixteen cases (94%) had no evidence of disease elsewhere in the body and the neoplastic process was not confined to regional salivary lymph nodes; therefore, these cases were considered primary extranodal lymphomas. One female patient (6%) reported a synchronous maltoma of the palate in conjunction with the parotid EMZBCL. Both lesions were noticed at the initial patient evaluation. It is unknown if the parotid gland lesion disseminated to the palate or if the palatal lesion manifested prior to the salivary gland lesion. Due to lack of complete medical history and the fact that EMZBCL manifests primarily in the major salivary glands instead of in minor salivary glands, it was assumed that the parotid lesion was most likely the primary site of the disease. Our study confirmed EMZBCL prevalence in females rather than males.[7, 13] However, it

showed a younger age of occurrence, during the fourth and fifth decades of life (Figure 7), rather than during the seventh decade of life as reported in the literature.[7, 13] This could be due to the size of our sample. The study demonstrated comparable incidence of EMZBCL in the major salivary glands, 88% in the parotid gland and 12% in the submandibular gland (Figure 6), as that reported by others, 75% in the parotid gland and 20% in the submandibular gland.[15, 20] It confirmed that EMZBCL of salivary glands occurs most often in the parotid gland.

All cases reviewed exhibited LELs with coalescing halos of monocytoid B-cells around them, a key feature of EMZBCL (Figures 8 and 9). The presence of halos are considered the "emergence" of EMZBCL in salivary gland[43] and the histomorphological "sign" at which monoclonality may first be detected.[49] The LELs were characterized by infiltration, distortion and destruction of the epithelium by the epitheliotrophic monocytoid B-cells. Even though effacement of the salivary gland parenchyma by lymphoid tissue was observed, the lobular architecture of the salivary gland was preserved. In all instances, monoclonality was demonstrated by κ light-chain restriction and/or IgH rearrangement. The two polyclonal cases were κ restricted and both demonstrated increased copy number of chromosome 3. The expression of IgH strongly supports a diagnosis of lymphoma.[39]

CD20 and CD79α demonstrated the B-cell lineage immunophenotype of the neoplastic cells (Figure 11). In five cases (29%), the aberrant co-expression of CD43/CD20 along with monoclonal immunoglobulin heavy chain rearrangement suggested a malignant lymphoproliferative neoplastic process.[50] Three of these cases

(60%) exhibited co-expression of CD43 in B-cells and κ light-chain restriction supporting a diagnosis of malignancy.[40] The equivocal result for CD43 in one case was most likely due to tissue degradation as a result of long-term storage. Cyclin D1, CD5 and CD23 failed to immunoreact in the monocytoid B-cells in all cases, ruling out a mantle cell lymphoma diagnosis (Figures 11 and 12). Lack of CD5/CD10 immunoreactivity differentiated a diagnosis of EMZBCL from other B-cell lymphomas.[40] CD10 was negative in all cases, ruling out a possible Burkitt's lymphoma (Figure 12). The lack of BCL2 positivity in the germinal centers in conjunction with lack of CD10 ruled out a follicular lymphoma diagnosis. Positive staining for CD20 along with lack of staining for CD5, CD10 and CD23 exclude the possibility of other small B-cell lymphomas such as small lymphocytic lymphoma/chronic lymphocytic leukemia, mantle cell lymphoma, and follicular lymphoma.[40] The ten cases (59%) with κ light-chain restriction confirmed that most B-cell neoplasms demonstrate a preference for κ restriction as opposed to λ restriction (Figure 13). Tissue and DNA degradation probably contributed to the remainder seven cases (41%) being inconclusive for light-chain restriction. The observed immunohistochemical profile in conjunction with the histomorphologic appearance and monoclonality confirms the diagnosis of EMZBCL in all reviewed cases.

Dual-color FISH highlights chromosomes without translocations with a yellow signal, indicating that the chromosomes have not broken apart at the spanning regions. A two fusion signal pattern reflects the two intact copies of the involved chromosome (Figure 14). When translocations occur, dual-color FISH displays separate red and green signals in addition to the yellow signal demonstrating the break apart points of the

chromosomes labeled with different probes (Figure 14). Furthermore, the presence of extra MALT1 break apart fusion signals (yellow) without separation is considered indicative of aneuploidy (abnormal number of chromosomes in a cell; complete or partial trisomy 3 and trisomy 18).[45, 51] Dual-color, dual fusion FISH demonstrates chromosomes without translocations with either a red or green signal, each corresponding to a different probe located on one particular chromosome (Figure 17). Cells in which chromosomes have translocations, dual-color-dual fusion FISH displays a yellow fusion signal as a result of fused probes located on separate chromosomes in addition to separate red and green signals (Figure 17). One of the main limitations with FISH performed on thin sections of paraffin-embedded tissue is that the paraffin and standard fixatives often times interfere with the hybridization process between DNA probes and the target loci.[52] Consequently, FISH signals may be decreased.

Our study failed to confirm reported 5% incidence of t(11;18)(q21;q21) in salivary glands .[1, 16, 31, 42, 46, 53] This was most likely due to the small sample size tested for API2/MALT1 gene rearrangement (2/17 cases). Even though our study could not corroborate the incidence of t(14;18)(q32;q21) in EMZBCL of salivary gland (16%)[1, 16, 30], it confirmed that t(14;18)(q32;q21) occurs with additional genetic abnormalities such as trisomy 3.[30] The only case demonstrating t(14;18)(q32;q21) IGH/MALT1 gene rearrangement in our study also showed increased copy number of chromosome 3 but not increased copy number of chromosome 18. However, it did not exhibit t(11;18)(q21;q21), which is consistent with previous reports stating that translocations observed in EMZBCL are mutually exclusive.[31, 46]

Chromosome enumeration probes (CEP) indicate increased copy number of the labeled chromosome by demonstrating more than two signals per cell. Our study confirmed that trisomy 3 is the most common genetic abnormality in EMZBCL of salivary glands as reported by others (Figure 15).[44, 46] It showed an overall incidence of 59% in contrast to 41% for increased copy number of chromosome 18 and 12% for MALT1 gene rearrangement. Such overall incidence was similar to that of trisomy 3 reported by Streubel et al (2004)[46] and Troch et al (2010)[44], 54.8% and 67% respectively. When presented as the sole genetic abnormality, increased copy number of chromosome 3 was still the most common genetic aberration noted. It showed an incidence of 24% in contrast to 12% for increased copy number of chromosome 18. The underlying mechanism for the prevalence of trisomy 3 in EMZBCL is unknown. It presumably involves increased transcription of an unknown tumor suppressor gene located in the short arm of chromosome 3 and/or aberrant expression of BCL6, located in chromosome region 3p27.[54]

Increased copy number of chromosome 18 (Figure 16) was demonstrated in 41% of our specimens (7/17), comparable to 40% overall incidence reported by Remstein et al (2006).[45] Streubel et al (2004) reported an overall incidence of 19% in EMZBCL of salivary glands.[46] Troch et al (2010) reported an overall incidence of 22% in EMZBCL of salivary glands.[44] When compared to our study, the incidence discrepancy seen with these other studies is most likely due to sample size. The sample size in Streubel's study was almost twice (42 cases) the size of the sample in our study (17 cases). The sample size used for genetic studies in Troch's study was half the size (9 cases) of the sample in

our study. Most cases in our study demonstrated concurrent increased copy number of chromosome 3 and chromosome 18, substantiating the claim that aneuploidy does not usually present as the sole genetic abnormality in EMZBCL of salivary glands. It is important to note that demonstrating increased copy number of a certain chromosome does not constitute irrefutable proof of trisomy. Cytogenetic studies are needed to unquestionably demonstrate trisomy of any given chromosome.

V. CONCLUSION

Our study adds seventeen EMZBCL cases of the major salivary glands to the body of literature necessary for proper characterization of such a rare entity. It substantiates immunohistochemical and molecular studies currently used to diagnose salivary EMZBCL. Furthermore, it serves as a control group to validate an ongoing study which evaluates previously diagnosed benign LESA lesions to determine which are consistent with salivary EMZBCL using current criteria. Even though EMZBCL is a low-grade lymphoma, it can disseminate and transform into a higher grade lymphoma such as DLBCL. The morbidity and mortality related to metastatic disease and high-grade lymphomas urges further study and characterization of EMZBCL to elucidate improved diagnostic techniques and treatment options. Differentiating between a benign lymphoproliferative process such as LESA and a malignant lymphoma will ensure proper treatment and improve patient outcome. Future studies should examine the incidence of t(1;14)(p22;q32) and t(3;14)(p14.1;q32) in salivary EMZBCL along with survival rates to determine if there is any correlation between observed genetic abnormalities and prognosis of such uncommon entity.

VI. REFERENCES

1. Jaffe E, Harris NL, Vardiman JW, et al. 2011. *Hematopathology*. Missouri: Elsevier. Pp. 106-108; 292-305.
2. Ihrler S, Harrison, J. Mikulicz's disease and Mikulicz's syndrome: analysis of the original case report of 1892 in the light of current knowledge identifies a MALT lymphoma. *Oral Surg, Oral Med, Oral Pathol, Oral Radiol Endod.* 2005; 100: 334-339.
3. Godwin J. Benign lymphoepithelial lesion of the parotid gland. *Cancer*. 1952; 1089-1103.
4. Schmid U, Helbron D, Lennert K. Development of malignant lymphoma in myoepithelial sialadenitis (Sjögren's syndrome). *Virchows Arch (Pathol Anat).* 1982; 395: 11-43.
5. Talal N, Sokoloff L, Barth WF. Extrasalivary lymphoid abnormalities in Sjögren's Syndrome (reticulum cell sarcoma, "pseudolymphoma", macroglobulinemia). *Amer J Med.* 1967; 43: 50-65.
6. Harris NL. Lymphoid proliferations of the salivary glands. *Amer J Clin Pathol*. 1999; 111(1 Suppl 1): S94-103.
7. Wenig, BM. 2016. *Atlas of Head and Neck Pathology*. 3rd ed. Philadelphia: Elsevier. Pp. 826-828, 837-841, 852-856, 1043-1048.
8. Thompson LDR, Wenig BM. 2013. *Diagnostic Pathology: Head and Neck Pathology*. Canada: Amirsys. Pp. 2: 40-43; 5: 4-7, 12-15, 52-53.
9. Ellis GL, Auclair PL. 2008. *AFIP Atlas of Tumor Pathology: Fascicle #9 Tumors of the Salivary Glands*. Washington DC: American Registry of Pathology. Pp. 136-141, 481-488.
10. Isaacson P. Mucosa-associated lymphoid tissue lymphoma. *Semin Hematol*. 1999; 36(2): 139-147.
11. Carbone A, Gloghini A, Ferlito A. Pathological features of lymphoid proliferations of the salivary glands: lymphoepithelial sialadenitis vs low-grade B-cell lymphoma of the MALT type. *Ann Otol, Rhinol Laryngol*. 2000; 109(12): 1170-1175.
12. Neville BW, Damm DD, Allen CM, et al. 2016. *Oral and Maxillofacial Pathology*. 4th ed. Missouri: Elsevier. Pp. 429-430.
13. Medeiros LJ, Miranda RN, Wang SA, et al. 2011. *Diagnostic Pathology: Lymph Nodes and Spleen with Extranodal Lymphomas*. Canada: Amirsys. Pp. 1:2-7; 6:24-29; 7:2-23, 44-53.
14. Zapater E, Bagán JV, Carbonell F, et al. Malignant lymphomas of the head and neck. *Oral Diseases*. 2010; 16: 119-128.
15. Nakamura S, Ichimura K, Sato Y, et al. Follicular lymphoma frequently originates in the salivary gland. *Pathol Int*. 2006; 56: 576-583.
16. Swerdlow SH, Campo E, Harris NL, et al (Eds). 2008. *WHO Classification of Tumors of Haematopoietic and Lymphoid Tissues.* France: International Agency for Research on Cancer (IARC). Pp. 214-226.

17. Yaprak N, Temel IC, Derin AT, et al. Diagnosis and treatment of malignant lymphomas of parotid gland. *Kulak Burun Bogaz Ihtis Derg*. 2015; 25(6): 346-349.
18. Triantafillidou K, Dimitrakopoulos J, Iordanidis F, et al. Extranodal Non-Hodgkin lymphomas of the oral cavity and maxillofacial region: a clinical study of 58 cases and review of the literature. *J Oral Maxillofac Sur.* 2012; 70: 2776-2785.
19. Shashidara R, Prasad PR, J, Joseph T. Follicular lymphoma of the submandibular salivary gland. *J Oral Maxillofac Pathol*. 2014; 18: 163-6.
20. Barnes L, Eveson JW, Reichart P, et al (Eds). 2005. *World Health Organization Classification of Tumors: Pathology and Genetics Head and Neck Tumors.* France: International Agency for Research on Cancer (IARC). Pp. 277-280.
21. Dabbs D. 2014. Chapter 6 Immunohistology of Non-Hodgkin lymphoma. *Diagnostic Immunohistochemistry: Theranostic and Genomic Applications.* 4th ed. Pennsylvania: Elsevier. Pp. 148-155, 159.
22. http://pathologyoutlines.com accessed on 15 September 2016.
23. Kojima M, Nakamura S, Ichimura K, et al. Follicular lymphoma of the salivary gland: a clinicopathological and molecular study of six cases. *Int J Surg Pathol*. 2001; 9(4): 287-293.
24. Lima MDM, Artico G, Soares FA, et al. Follicular lymphoma in the palate with clinical appearance similar to salivary gland tumors. *Quintessence Int*. 2010; 41: 661-663.
25. Azzopardi JG, Evans DJ. Malignant lymphoma of parotid associated with Mikulicz disease (benign lymphoepithelial lesion). *J Clin Pathol*. 1971; 24: 744-752.
26. Nime F, Cooper H, Eggleston J. Primary malignant lymphomas of the salivary glands. *Cancer*. 1979; 37: 906-912.
27. Isaacson P, Wright DH. Malignant lymphoma of mucosa-associated lymphoid tissue: a distinctive type of B-cell lymphoma*. Cancer*. 1983; 52: 1410-1416.
28. Isaacson PG, Wright DH. Extranodal malignant lymphoma arising from mucosa-associated lymphoid tissue. *Cancer.* 1984; 53: 2515-2524.
29. Harris NL, Jaffe ES, Stein H, et al. A Revised European-American classification of lymphoid neoplasms: a proposal from the International Lymphoma Study Group. *Blood.* 1994; 84(5): 1361-1392.
30. Streubel B, Lamprecht A, Dierlamm J, et al. t(14;18)(q32;q21) involving IGH and MALT1 is a frequent chromosomal aberration in MALT lymphoma. *Blood*. 2003; 101(6): 2335-2339.
31. Ferry, J. Extranodal lymphoma. *Arch Pathol Lab Med*. 2008; 132: 565-578.
32. Abbondanzo S. Extranodal marginal-zone B-cell lymphoma of the salivary gland. *Ann Diagn Pathol*. 2001; 5(4): 246-254.
33. Ambrosetti A, Zanotti R, Pattaro C, et al. Most cases of primary salivary mucosa-associated lymphoid tissue lymphoma are associated either with Sjögren syndrome or hepatitis C virus infection. *Br J Haematol*. 2004; 126:43-49.
34. Khalil MO, Morton LM, Devesa SS, et al. Incidence of marginal zone lymphoma in the United States, 2001-2009, with a focus on primary anatomic site. *Br J Haematol*. 2014; 165: 67-77.

35. Kassan SS, Thomas TL, Moutsopoulos HM, et al. Increased risk of lymphoma in sicca syndrome. *Ann Intern Med.* 1978; 89(6): 888-892.
36. Zucca E, Conconi A, Pedrinis E, et al. Nongastric marginal zone B-cell lymphoma of mucosa-associated lymphoid tissue. *Blood.* 2003; 101: 2489-95.
37. Wöhrer S, Troch M, Streubel B, et al. Pathology and clinical course of MALT lymphoma with plasmacytic differentiation. *Ann Oncol*. 2007; 18: 2020-2024.
38. Rosenwald A, Ott G, Stilgenbauer S, et al. Exclusive detection of the t(11;18)(q21;q21) in extranodal marginal zone B-cell lymphomas (MZBL) of MALT type in contrast to other MZBL and extranodal large B-cell lymphomas. *Am J Pathol*. 1999; 155:1817-21.
39. Rawal A, Finn W, Schnitzer B, et al. Site-specific morphologic differences in extranodal marginal zone B-cell lymphomas. *Arch Pathol Lab Med*. 2007; 131: 1673-1678.
40. Wang G, Auerbach A, Wei M, et al. t(11;18)(q21;q21) in extranodal marginal zone B-cell lymphoma of mucosa-associated lymphoid tissue in stomach: a study of 48 cases. *Mod Pathol*. 2009; 22: 79-86.
41. Campo E, Swerdlow S, Harris N, et al. The 2008 WHO classification of lymphoid neoplasms and beyond: evolving concepts and practical applications. *Blood*. 2011; 117 (19): 5019-5032.
42. Auer IA, Gascoyne RD, Connors JM, et al. t(11;18)(q21;q21) is the most common translocation in MALT lymphomas. *Ann Oncol*. 1997; 8: 979-85.
43. Bacon C, Du M, Dogan A. Mucosa-associated lymphoid tissue (MALT) lymphoma: a practical guide for pathologists. *J Clin Pathol*. 2007; 60: 361-372.
44. Troch M, Formanek M, Streubel B, et al. Clinicopathological aspects of mucosa-associated lymphoid tissue (MALT) lymphoma of the parotid gland: a retrospective single-center analysis of 28 cases. *Head Neck.* 2010; 33: 763-767.
45. Remstein ED, Dogan A, Einerson RR et al. The incidence and anatomic site specificity of chromosomal translocations in primary extranodal marginal zone B-cell lymphoma of mucosa- associated lymphoid tissue (MALT lymphoma) in North America. *Am J Surg Pathol.* 2006; 30; 1546-1553.
46. Streubel B, Simonitsch-Klupp I, Mullauer L et al. Variable frequencies of MALT lymphoma-associated genetic aberrations in MALT lymphomas of different sites. *Leukemia.* 2004; 18; 1722-1726.
47. Reed TJ, Reid A, Wallberg K, et al. Determination of B-cell clonality in paraffin-embedded lymph nodes using the polymerase chain reaction. *Diagn Mol Pathol.* 1993; 2: 42-49.
48. Wan JH, Trainor KJ, Brisco MJ, et al. Monoclonality in B-cell lymphoma detected in paraffin wax embedded sections using the polymerase chain reaction. *J Clin Pathol.* 1990; 43: 888-890.
49. Diss T, Wotherspoon A, Speight P, et al. B-Cell Monoclonality, Epstein Virus and t(14;18) in Myoepithelial Sialodenitis and Low-Grade B-Cell MALT Lymphoma of the Parotid *Gland. Am J Surg Pathol.* 1995; 19 (5): 531 - 536.
50. Hsi E, Zukerberg L, Schnitzer B, Harris N. Development of Extrasalivary Gland Lymphoma in Myoepithelial Sialadenitis. *Mod Pathol*. 1995; 8: 817–24.

51. Kobayashi Y, Nakata M, Maekawa M, et al. Detection of t(11;18) in MALT-Type Lymphoma with Dual-Color Fluorescence In Situ Hybridization and Reverse Transcriptase-Polymerase Chain Reaction Analysis. *Diag Mol Pathol*. 2001; 10(4): 207-213.
52. Paternoster SF, Brockman SR, McClure RF, et al. A New Method to Extract Nuclei from Paraffin-Embedded Tissue to Study Lymphomas Using Interphase Fluorescence in Situ Hybridization. *Am J Pathol*. 2002; 160 (6): 1967-1972.
53. Harris NL, Isaacson PG. What are the Criteria for Distinguishing MALT from Non-MALT Lymphoma at Extranodal Sites? *Am J Clin Pathol*. 1999; 111(1 Suppl 1):S126-32.
54. Wotherspoon AC, Finn TM, Isaacson PG. Trisomy 3 in Low-grade B-Cell Lymphomas of Mucosa-Associated Lymphoid Tissue. *Blood*. 1995; 85(8): 2000-4.